Northern Sea Otter (*Enhydra lutris kenyoni*) Population Abundance and Distribution across the Southeast Alaska Stock
Summer 2022

USFWS Region 7 Technical Report MMM 2023-01
March 2023

Cover Images: Example imagery from photo-based sea otter population surveys in Southeast Alaska in summer 2022. Sea otters were detected in canopy kelp, (top), in open water (bottom), and other settings using two independent imaging systems attached to an airplane flying designated transects across the region.

Paul Schuette[1], Joseph Eisaguirre[2], Benjamin Weitzman[1]
Collin Power[1], Evan Wetherington[1], Jenipher Cate[1], Jamie Womble[3], Linnea Pearson[3], Daniel Melody[4], Chelsea Merriman[4], Kat Hanks[4], George Esslinger[2]

[1] U.S. Fish and Wildlife Service
Marine Mammals Management
Region 7, Alaska
1011 E. Tudor Road
Anchorage, Alaska 99503

[2] U.S. Geological Survey
Alaska Science Center
4210 University Drive
Anchorage, Alaska 99508

[3] National Park Service
Southeast Alaska Inventory & Monitoring Network
3100 National Park Road
Juneau, Alaska 99801

[4] Owyhee Air Research
3305 Airport Rd
Nampa, Idaho 83687

Contents

Executive Summary

In the summer of 2022, the U.S. Fish & Wildlife Service and partners successfully completed the first single-year, aerial photo survey of sea otters across the entire Southeast stock of northern sea otters. This document presents the latest findings from the 2022 Southeast Alaska Sea Otter Survey, providing up-to-date information regarding occupancy, abundance and carrying capacity. We collected two independent data streams of sea otter observations during the survey using novel image sensor technologies for marine wildlife surveys and recently developed statistical methods. We calculated an abundance estimate of 22,359 (95% Bayesian credible interval: 19,595, 25,290, CV = 0.064) sea otters. Based on these results, the population size of the Southeast stock of northern sea otters is still increasing and below the estimated carrying capacity for the region of 48,083 (95% Bayesian credible interval: 40,575, 58,570) sea otters. Results from this report include the first updated abundance estimates for the Southeast stock of sea otters in 10 years, which will help inform stakeholders from across the region and addresses the top priority identified by the 2019 Southeast Sea Otter Stakeholder Working Group.

1. Background and Objectives

1.1 Background

Northern sea otters (*Enhydra lutris kenyoni*) in Alaska are managed by the U.S. Fish & Wildlife Service, Marine Mammals Management under the Marine Mammal Protection Act as three distinct stocks (Gorbics and Bodkin 2001) (Figure 1). The Southeast stock extends from Dixon Entrance in the south to Cape Yakataga at the north (Figure 2). The region includes more than 1,100 islands of the Alexander Archipelago and mountainous, forested terrain on the mainland. The physical and environmental conditions on land and in coastal waters are highly productive, evident in the diverse ecosystems that have supported sea otters and coastal Indigenous communities for over ten thousand years (Fedje et al. 2005).

Archaeological evidence indicates sea otters were harvested by coastal Indigenous Peoples primarily for their fur rather than consumption (Moss 2020). Coastal Indigenous Peoples also harvested many of the same benthic invertebrates (e.g. clams, mussels, abalone, chitons, sea urchins) consumed by sea otters (Szpak et al. 2012). Thus, localized sea otter harvests may have incurred benefits to Indigenous Peoples not only for their pelts, but also to alleviate sea otter predation pressure on invertebrates thereby increasing local availability of those food sources (Salomon et al. 2015). A network of low-density human population centers and localized harvest practices, as well as spatial variability in the nearshore environment, likely resulted in a gradient of sea otter density across the region and relatively stable ecosystem states for millennia (Estes and Duggins 1995).

The dynamics of sea otter populations started to change as Russian fur traders, and eventually, western European and American merchants, targeted sea otters for their pelts. Sea otter harvest in support of the fur trade started in the 15th century and expanded following Russian voyages in the 18th century (Bodkin 2015). By 1890, sea otters had been virtually extirpated from Southeast Alaska, except for a few unconfirmed individuals scattered across the region (Kenyon 1969). Sea

otters across their historical range from eastern Asia to North America were nearing extinction by the end of the 19th century. At that time, the global population of sea otters, which once likely numbered 100,000 - 150,000 otters, had been reduced to potentially fewer than 2,000 animals spread across 13 remnant colonies (Kenyon 1969).

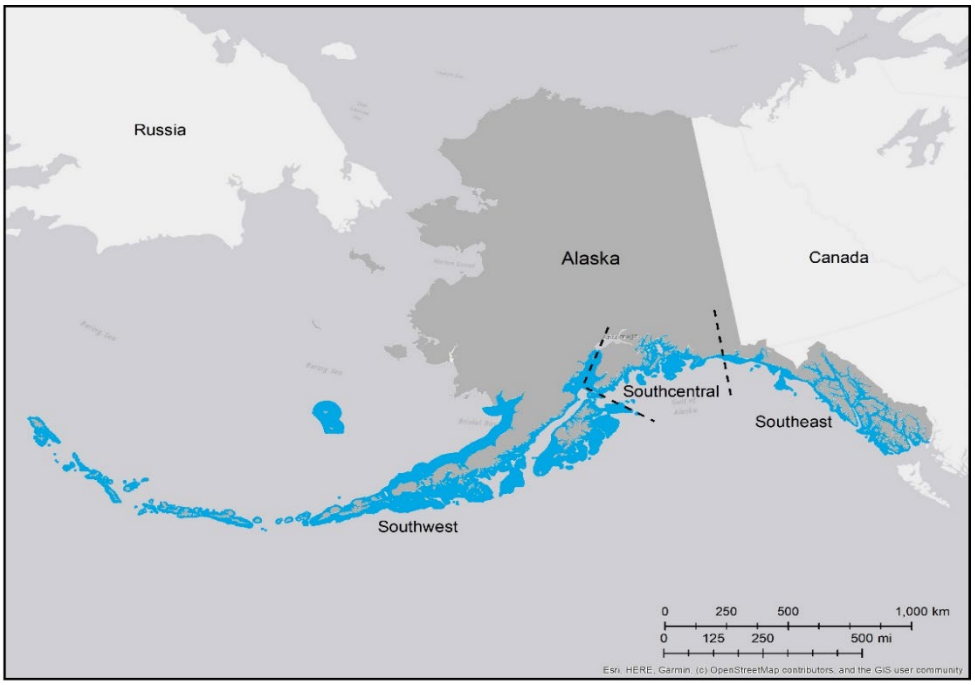

Figure 1. Northern sea otter stock distribution in Alaska (blue), delineated as ocean waters within the 100 m (328 ft) depth contour, within the median ice extent for the month of March from 2001 – 2020, and restricted to the 24 nautical mile Contiguous Zone maritime boundary. The boundaries among the three stocks are indicated with a dashed line.

The International Fur Seal Treaty of 1911 ended the international sea otter fur trade and subsequently, sea otter populations naturally grew and repatriated historic habitats from 13 remnant colonies across their historic range (Bodkin 2015). Following Alaska statehood, from 1965 - 1972 the Alaska Department of Fish and Game (ADF&G) reintroduced northern sea otters to several areas where they had been extirpated but had not yet naturally recolonized Southeast Alaska, Washington, and Oregon. This effort included translocation of 413 otters mixed together from sea otter populations in Prince William Sound and Amchitka Island to seven locations in Southeast Alaska (Jameson et al. 1982). The passage of the Marine Mammal Protection Act in 1972 provided additional protection to sea otters and all other marine mammals occurring in U.S. waters. Alaska Native community members from coastal-dwelling tribes were provided an exemption that allows sea otter harvest for subsistence and for alteration of sea otter pelts for preparation and sale of traditional handicrafts. Passage of the Alaska Native Claims Settlement Act (ANCSA) of 1971 and the Alaska National Interest Lands Conservation Act (ANILCA) in 1980 further transformed the land and seascape of Alaska.

Following implementation of legal protections and reintroductions, sea otters started to recolonize areas where they had been absent for nearly a century. During the period of sea otter

absence, their prey had increased in size and abundance, likely due to a release from intense predation (Tegner and Dayton 2000). The absence of sea otters corresponded with abundant shellfish (e.g., sea urchins, sea cucumbers, mussels, clams, crab, chitons) that supported commercial and personal-use shellfisheries, rural subsistence users, and influenced the ecosystem structure of nearshore habitats (Estes and Duggins 1995). Abundant shellfish also facilitated sea otter population growth, which created conflict with commercial fisheries and threatened food security for coastal communities across the region (Hoyt 2015, Ibarra 2021). Despite conflicts, sea otter hunters and artisans benefited from having restored access to sea otter fur for trading, making handicrafts, and generating income, and the presence of sea otters near communities has also created ecotourism opportunities (Burt et al. 2020). The ecosystem services provided by an ecologically functional sea otter population can also broadly benefit communities with potentially increased finfish availability and productivity, carbon sequestration, and climate change mitigation (Wilmers et al. 2012, Gregr et al. 2020, Rasher et al. 2020).

In response to the growing challenges of increased number of sea otters for communities throughout Southeast Alaska, the U.S. Fish & Wildlife Service, Marine Mammals Management (hereafter, USFWS) formed the Southeast Sea Otter Stakeholder Working Group in November 2020 following an in-person stakeholder workshop held in Juneau, Alaska in November 2019. The effort brought together federal Department of Interior (DOI) agencies, state agencies, academic scientists, tribal and community representatives, commercial fisheries representatives, conservation non-profit organizations, and other stakeholders to promote open dialogue and work towards a future of coexistence between humans and sea otters. One of the top priorities identified at the workshop was the need for new sea otter population survey data to provide a current estimate of sea otter abundance and distribution across Southeast Alaska, which had not been attempted since a two-year survey in 2010 and 2011 (USFWS 2020).

1.2 Historical Surveys

The USFWS and its DOI partners at the National Park Service (NPS) and U.S. Geological Survey (USGS) have conducted periodic sea otter population surveys to track population trends and harvest across Southeast Alaska. Aerial, observer-based surveys of sea otters have been conducted across subsets of Southeast Alaska over the past three decades. Yakutat Bay was surveyed in 1995 and 2005. The remainder of Southeast Alaska, excluding Glacier Bay, was surveyed in 2002/03 and 2010/11 (Esslinger and Bodkin 2009, Esslinger 2020). These aerial surveys involved an observer flying in a single–engine fixed-wing aircraft at an altitude of 90 meter [m] (~300 feet [ft]) and a speed of approximately 120 kilometers per hour [kph] (~ 65 knots [kts]) to survey 400 m (0.25 mi) wide transects. Each survey was designed to meet the assumptions of a design-based abundance estimator, which included a survey specific correction factor to account for sea otter availability (e.g. sea otters diving or foraging underwater) and detectability (e.g. observer ability to detect sea otters on the water's surface) (Bodkin and Udevitz 1999). The correction factor was estimated by utilizing Intensive Search Units (ISU) during the design-based surveys (Bodkin and Udevitz 1999). These methods were consistently used as the standard for sea otter surveys throughout the Gulf of Alaska for nearly 25 years (Esslinger et al. 2021).

Semi-annual distribution and design-based surveys have been conducted in Glacier Bay National Park and Preserve (hereafter, Glacier Bay) since 1993 by NPS and the USGS. Distribution surveys were conducted in 1993, 1996 – 1998, 2005, 2009, and 2010 using multiple aircraft platforms flown at an altitude of approximately 150 m (~500 ft) at 165 kph (~90 kts) wherever sea otters were expected to occur at the time. Design-based surveys using the ISU method were conducted 1999 - 2004, 2006, and 2012 (Esslinger et al. 2015, Esslinger 2019). These surveys were integrated with historical data to reveal population growth and range expansion in Glacier Bay over a twenty-year period (1993 – 2012) (Williams et al. 2019).

Beginning in 2017 in Glacier Bay, survey methods transitioned from the traditional surveys (Bodkin and Udevitz 1999) to optimized photo-based methods, increasing the safety and efficiency of surveys while also providing a permanent record of what was observed. This design involved random transects, optimized transects, and transects chosen based on model predictions of high population densities (Womble et al. 2018). Statistically optimized transects were placed based on local environmental conditions, logistical constraints, and forecast densities of sea otters (Williams et al. 2018). This photo-based method was flown in a single-engine high-winged, float-equipped aircraft. The aircraft flew at an altitude of 213 – 250 m (705 – 820 ft) and a speed of 157 - 166 kph (~ 85 – 90 kts). Digital photographic images were taken with a single, Nikon D810 camera (36.3MP) with an 85 millimeter [mm] Zeiss lens. These flight and image capture parameters resulted in a ground sampling distance (GSD) resolution of 1.23 centimeter [cm] per image pixel (Womble et al. 2018).

The NPS Southeast Alaska Network provided a time series of data and abundance estimates through 2019 (Womble et al. 2020). While the remainder of the Southeast Alaska region had not been surveyed since a two-year effort in 2010 and 2011, reanalysis of information provided updated estimates of abundance for the Southeast stock of 25,584 sea otters in 2011 and a total predicted carrying capacity of 74,650 sea otters (Tinker et al. 2019). Modern mechanistic spatiotemporal models (Hefley et al. 2017) that allow integration of multiple types of disparate survey data have informed the overall stock abundance through 2019, providing an updated stock assessment for the Southeast stock of 27,285 sea otters and an updated estimate of carrying capacity at 62,542 (90% Bayesian credible interval: 54,063, 89,922) sea otters (Eisaguirre et al. 2021, 2023). However, none of these recently published estimates were generated from updated empirical observations outside of Glacier Bay and the cost in time and funding for surveying sea otters using traditional methods had become prohibitive for large-scale efforts such as surveying the entire Southeast stock. To collect more recent survey data at such a large scale, there was a need to increase the safety and efficiency of aerial surveys, as demonstrated in Glacier Bay (Womble et al. 2018), more broadly across the region.

1.3 Objectives

Our primary objectives as recommended by the Southeast Sea Otter Stakeholder Working Group were the following:

1) Provide a current estimate of sea otter abundance and distribution for the Southeast stock.

2) Provide a current estimate of predicted sea otter carrying capacity for the Southeast stock.

To accomplish these primary objectives, we also aimed to achieve the following methodological advances to improve the efficiency, reliability, and safety of sea otter population monitoring strategies:

1) Develop an optimized survey design that would allow USFWS to conduct a population survey spanning the entire stock in a single year and produce estimates of abundance and carrying capacity with high precision.

2) Adopt photo-based methods, including use of imaging/video-based systems, artificial intelligence algorithms, and development of data management workflows, to detect sea otters during the survey and archive data for future use.

2. Methods

2.1 Study Area

2.1.1. Region Overview

The study area encompasses approximately 90,000 square kilometers (km^2) (34,749 square miles) extending from Cape Yakataga in the north to the southern extent of the stock at Dixon Entrance (Figure 2). For the survey, we considered all coastal waters in the Southeast stock including islands and mainland extending up to 10 km from outer coast shorelines or the 100 m isobaths, whichever was further from the outer coast shore. USFWS and Owyhee Air Research led survey efforts for all coastal waters except for Glacier Bay, which was led by NPS biologists concurrent with the regional USFWS effort.

2.2 Survey Design

2.2.1 Optimized Design

We followed recent advances in designing sea otter surveys in Glacier Bay and implemented a statistical survey optimization procedure to maximize the utility of the data collected over such a large survey area and to efficiently survey a growing and expanding population of sea otters (Williams et al. 2018, Womble et al. 2018, Leach et al. 2022). We first applied the dynamic spatiotemporal model presented by Eisaguirre et al. (2021), which was fit to all available aerial survey data in Southeast Alaska through 2019 to create a statistical forecast of sea otter abundance across the stock region for 2022. We then proposed 1,000 candidate survey designs by randomly placing lateral transects across the region, each totaling ≤ 6,500 km (~ 4,039 mi) of transect distance. Next, we refit the model to the forecast data collected following each candidate design using recursive Bayesian computation (Leach et al. 2022). Given the importance of both abundance and carrying capacity to the management of sea otters under the MMPA, we chose to optimize the survey design based on a quantity termed equilibrium differential, which is computed as the difference between estimated local carrying capacity and abundance (Eisaguirre et al. 2023). Finally, for each design, we estimated equilibrium differential and chose the survey design that maximized the precision of the estimate of total equilibrium differential. The chosen design improved precision by 36% over the average design. The total length of the optimized transects was 5,483 km (3,407 mi), spaced at variable distances based on the optimization

procedure, with a minimum spacing between transects of 400 m (0.25 mi), due to the 400 m^2 grid cell structure used to create transects.

Sea otter surveys from 2017 - 2019 in Glacier Bay consisted of three survey strata, optimized transects, abundance transects, and randomized transects (Womble et al. 2018), conducted during July and August. These 3 strata were combined in an integrated population model for Glacier Bay to provide precise and accurate estimates of abundance within Glacier Bay for 2017 - 2019 (Womble et al. 2018). In August 2022, these three strata were combined, summing to 903 km (561 mi) of transects, and were added to the survey dataset used to estimate abundance for the entire stock region, which was similarly done by Eisaguirre et al. (2021; 2023) with the 2017-2019 data.

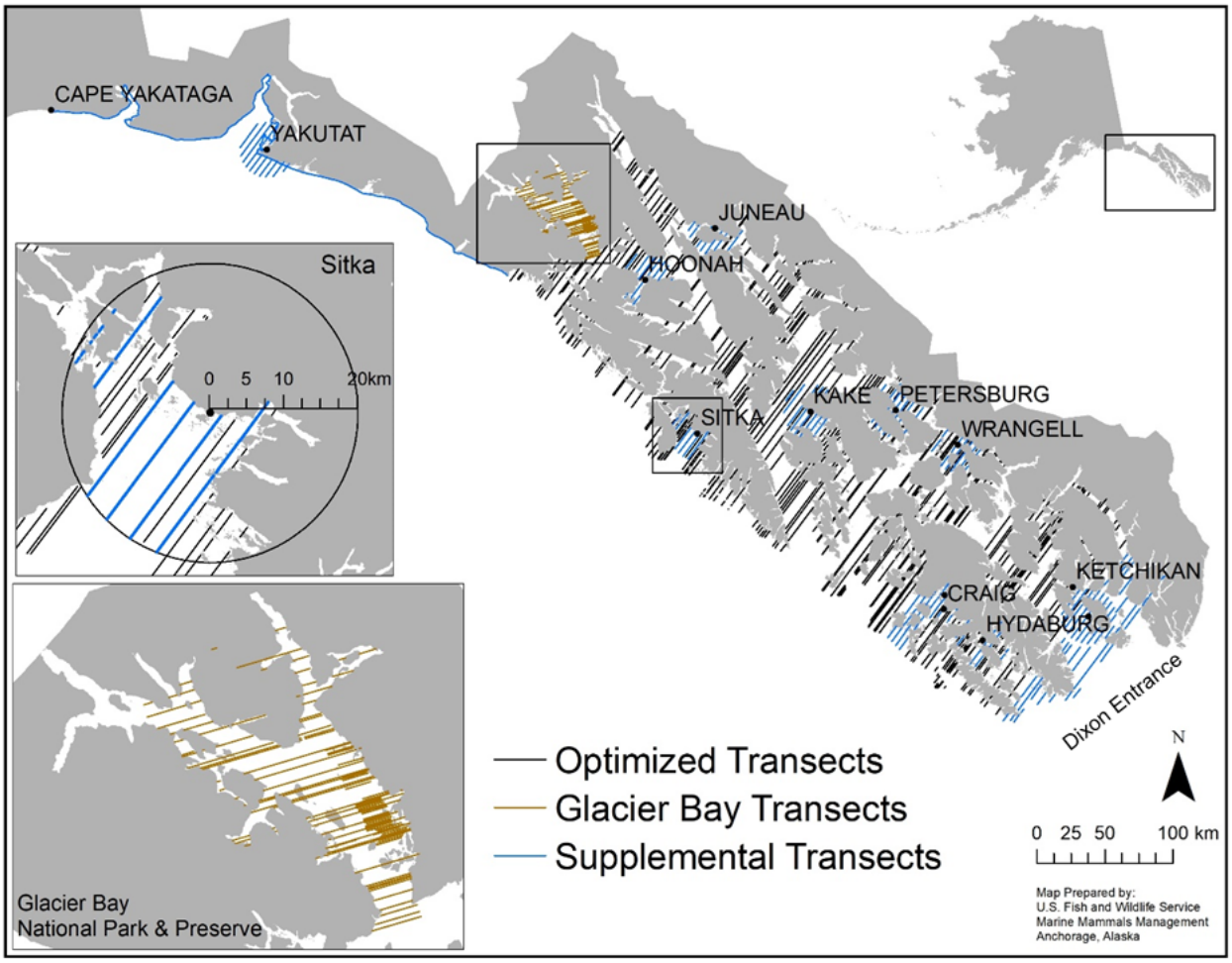

Figure 2. Aerial survey design for the 2022 Southeast Alaska sea otter population survey. The photo-based survey study design included optimized transects supplemented with additional transects around 10 focal communities (e.g., Sitka, top left inset) within 20 km of the location and expert opinion. Surveys of Glacier Bay National Park and Preserve (lower left inset) were conducted by the National Park Service in August 2022 and included three transect strata.

2.2.2 Supplemental Transects

We supplemented the optimized survey design to improve our understanding of the sea otter population in areas of high interest to Southeast stakeholders (Figure 2). First, we increased survey coverage around 10 human population centers, including (in alphabetical order): Hoonah, Hydaburg, Juneau, Kake, Ketchikan, Klawock, Metlakatla, Petersburg, Sitka, Wrangell, and Yakutat. Using spatial tools in ArcMap 10.7.1 (ESRI 2019), we created a 20 km buffer around each location's center. We then systematically added transects parallel to the optimized transects within the buffer area to ensure we achieved transect coverage of ≤ 4 km (2.5 mi) separation among transects surrounding each community (Figure 2). Supplemental transects contributed an additional 1,069 km (664 mi) to the optimized design. Second, we added 576 km (358 mi) of transect parallel to the coast extending from Palma Bay to Cape Yakataga along the outer coastal of Southeast Alaska. This coastal transect provide coverage of nearshore waters in an area that has not been surveyed by air since 2005, but was expected to contain low densities of sea otters (Gill and Burn 2007). Third, we added 340 km (211 mi) of transect to an area south of Ketchikan and Metlakatla to fill an information gap identified by USFWS and USGS which was not covered by the optimized design and fell outside of the community buffer areas. Fourth, we shared details of the study design and a map of the transects (that included optimized transects and supplemental transects) with members of the Southeast Sea Otter Stakeholder Working Group in advance of the survey to request feedback and recommendations for additional areas to survey. We received one comment, which requested we add transects around Baker, Noyes, and Lulu islands in an area on the outer coast west of Klawock and Craig. We added 114 km (71 mi) of transects in this area.

The combination of optimized transects and supplemental transects resulted in a total of 7,471 km (4,642 mi) of transect to be surveyed by USFWS, complemented by 903 km (561 mi) of transect surveyed by NPS in Glacier Bay (Figure 2).

2.3 Field Methods for Sea Otter Aerial Photographic Survey

The aerial photographic survey was flown by Owyhee Air Research (OAR; Nampa, Idaho) using a Partenavia P68C, a light twin-engine, fixed-wing aircraft. Surveys were flown at approximately ~150 kph (80 kts; up to 100 kts when there was a strong tailwind) and at an altitude of 214 m (range: 183 m - 267 m; 700 ft, range: 600 - 875 ft) above sea level (ASL). The surveys were flown with a three-person flight crew consisting of one pilot, one OAR camera operator, and one USFWS biologist operating a second camera sensor. The survey was conducted during daylight hours for up to 8 hours per day from approximately 8 am - 8 pm (0800 to 2000 AST), dependent on weather and glare conditions. The survey team strategically based out of Juneau, Sitka, Petersburg, and Ketchikan during the survey over a 4 - week period in May and June to limit transit times. Brief stopovers were made at Klawock, Gustavus, and Skagway.

Transects were flown end-to-end following the designated transect design, which were preloaded on to the pilot's Apple iPad (Cupertino, CA) in the ForeFlight iOS (Houston, TX) app. The flight path was monitored by the pilot and observers, checking off transects as the survey was completed, generally from the north part of the study area working to the south. Some designated transects (< 1%) were not surveyed due to safety factors such as dangerous topography in narrow

fjords and turbulent weather. When weather conditions were deemed sub-optimal (e.g., surface chop on the water, swell, or destabilizing winds at altitude), surveys were paused until conditions improved or the flight crew flew into workable conditions.

Photographic surveys utilized two independent imaging systems: 1) a L3/Harris MX-10 EO/IR multi-sensor videographic imaging system (Melbourne, FL) paired with a dedicated Churchill Navigation/Shotover Systems (Boulder, CO) augmented reality system (ARS) computer supplied and operated by OAR; and 2) a Waldo XCam Ultra50 photogrammetric imaging system (Thompsons Station, TN) provided and operated by USFWS across Southeast Alaska and NPS within Glacier Bay. Across Southeast Alaska both imaging systems were used simultaneously to acquire two independent data streams that could be used for analysis and to provide redundancy in case one of the sensors experienced technical difficulties.

2.3.1 L3/Harris MX-10 Imaging System: Infrared and Color Video

The majority of the survey (except Glacier Bay, see below) was flown using a belly mounted MX-10 imaging system (see Appendix 3, Figure A3.1 for pictures). The MX-10 acts as an observer-based system in which an operator continuously views a monitor with a live video stream with full operational control of the infrared (IR) and red-green-blue (RGB) sensors in-flight. This dual sensor system allowed us to search for animal 'heat signatures' and confirm species identities with the super high-resolution RGB video imagery with zoom capabilities. Preliminary testing of the MX-10 at Pleasant Island, an area known to be occupied by sea otters, was flown on the first day in the field to allow the camera operator to calibrate the MX-10 system for sea otters. Once calibrated, sea otters displayed a clear (heat) signature in IR imagery, allowing them to be easily located against a background of ocean water or coastal terrain.

The standard operating procedure included the camera operator scanning a fixed width area of 345 m (0.21 mi) using IR. For every potential sea otter, the operator would switch to the high resolution RGB video to confirm whether the object(s) were sea otters. When a heat source was identified as a sea otter, the operator recorded two screenshots of the positive identification, one in IR and one in RGB. Detected otters were tagged with a georeferenced marker on the ARS computer for counting and geolocation purposes. The date and time were recorded, and all other information recorded on the ground during post-processing. Any groups (i.e., sea otters clustered < 5 body lengths apart) larger than ten were counted post-flight. We recorded the age composition of observed sea otters as adults and pups when > 1 otter was detected based on relative body sizes. Lone sea otters were recorded as adults. Sea otters in very large groups or at a great distance were not classified as adults or pups, and only a final total count was provided.

Although double counting is a concern for any wildlife survey, OAR's technology and procedures minimize those risks during aerial IR surveys. Processes to reduce the probability of double counting were incorporated into the survey protocol. In-flight geospatial software allowed the operator to mark each detected individual with a georeferenced marker, which were saved at the end of each flight. At the beginning of each flight, detection points from the prior flight were loaded into the ARS system before take-off and used to identify previously observed detection locations and densities. This survey was conducted in a manner to further minimize the probability of double counting by flying transects in the same sampling region until completion,

unless poor weather prevented completion, in which case the survey was continued at a later date. Additionally, the pilot and USFWS biologist in the plane coordinated to complete sections of survey that utilized topographic barriers that would naturally prevent sea otter movement within the short time period of the survey.

2.3.2 Intensive Searches to Estimate Availability

Throughout the survey, OAR and USFWS were able to complete 29 intensive searches of sea otter groups to estimate the proportion of sea otters that were 'available' for detection. Sea otters forage underwater for usually around 1 minute on average though dives as long as 7.9 minutes have been documented (Thometz et al. 2016). During a traditional survey, observers would periodically conduct ISUs, 400 m (0.25 mi) diameter circles at a specific speed, covering the same area of water to develop a correction for availability. We adapted this approach but with the MX-10 video imaging system to make statistical inferences regarding how many otters were 'available' (i.e., readily photographed on the surface of the water or on land) vs. 'unavailable' (i.e., otters underwater that could not be seen during the initial flight over the otter group).

Intensive searches of sea otter groups were determined in advance at random by the USFWS biologist up to 3x per day to spread the intensive searches across variable habitat conditions and time of day. An intensive search was conducted when the USFWS biologist on board announced that the next sea otter observed would trigger an intensive search. Intensive searches consisted of the plane increasing its altitude to approximately 305 m (1,000 ft) and then circling the detected otter group for 5 minutes recording video throughout of an area of approximately 98 - 197 m (322 - 646 ft). All sea otters that came into view (except sea otters that swam in from outside the area) during those five minutes, after the initial target sea otter(s), were counted and the additional number recorded on the data sheet. We therefore had a record of the initial count of sea otters detected and a second count that included the initial count plus the count of animals that surfaced during the 5-minute intensive search.

2.3.3 Waldo XCam Ultra 50 Imaging System: Color Images

The Waldo XCam Ultra 50 is a lightweight camera pod (~ 4.5 kg; 9.9 pounds) consisting of two full size Cannon 5DS R 50.6 MP RGB cameras with fixed-zoom 50mm f/1.4 lens, an integrated GPS unit, and micro-controller to trigger capture events. The two cameras in the pod were synchronized by Waldo software and programmed to continuously capture images throughout the flight. The Waldo XCam is an image acquisition strategy (rather than observer-based) that only requires a camera operator for adjusting the camera settings (e.g., F-stop, ISO, exposure) in flight. The Waldo camera pod was attached to the strut of a Cessna 206 for Glacier Bay and on the belly of the OAR P68C in an existing port under the front passenger seat for the broader Southeast Alaska region. During surveys, either a NPS or USFWS biologist operated the camera to ensure the camera was functioning properly and image quality was satisfactory (e.g., not under/over exposed). While flying on transect, the camera continuously recorded images. The interval between images was limited by the USB transfer speed, averaging ~ 1.5 seconds between capture events. The width of each captured image while flying 120 - 148 kph (65 - 80 kts) at 213 m (700 ft) altitude was ~ 300 m (984 ft). Target resolution of Waldo imagery was 1.77 cm/pixel. Photos were captured in manual mode based on several preset profiles with values

between ISO 400 - 800, f/2.4 - f/5.6, and shutter speed between 1/2500 - 1/5000 seconds. These profiles were generated from test flights conducted prior to the Southeast survey to optimize image clarity and exposure in a range of environmental conditions.

The swath width of the Waldo XCam was comparable to the MX-10 swath width, but the Waldo XCam provided a nadir, instantaneous snapshot and the MX-10 provided a trapezoidal video viewshed lasting for several seconds, and recorded observations of the same space, 30 seconds after the Waldo's image capture. In both data streams, the imagery was recorded throughout the survey for review after each flight, and a permanent record was copied and archived for future use. The platforms differed substantially in the amount of post-flight processing and data management prior to statistical analyses. Whereas the MX-10 data was collected in-flight and reviewed after the flight to record and update sea otter counts, the Waldo XCam images were not evaluated until after each day's flight. We developed an Artificial Intelligence (AI) algorithm to automate the process of identifying images that potentially contained sea otters and used a manual validation process to confirm species identity and generate counts from each photo (see data management below).

2.4 Data Management

2.4.1 L3 Harris/MX10: Color and Infrared Video Observer – Based Sea Otter Detections

We backed up all recorded video, screenshot images, aircraft GPS tracks, and viewing area of the MX-10 (i.e., search effort) onto external hard drives with triple redundancy each day. We conducted quality assurance and quality control each evening by reviewing IR and RGB video to confirm or update sea otter counts recorded in flight and to add any additional details from the observation, such as GPS coordinates, time-date information, and video file identification.

We created a sea otter detection spreadsheet in Microsoft Excel with all sea otter observations, including total counts distinguished as adults and pups, GPS coordinates, time, date, and video file name. The spreadsheet included details on the subset of sea otter detections in which intensive searches were conducted to estimate availability. We also exported all geospatial data, which included GPS track lines of each transect flown, transit flights, and GPS locations of sea otters detected on transect as a final clean data set for statistical population modeling.

2.4.2 Waldo XCam Ultra 50: Artificial Intelligence Assisted Sea Otter Detections

We used *SeeOtter,* a custom software program we developed for this project, to process Waldo XCam images with our AI model and manually validate the processed imagery. Computationally, *SeeOtter* facilitates the application of AI models to photo-survey data to provide ready to process output for our statistical population models. We built a custom-trained YOLOv5 object detection AI model (Jocher et al. 2022) using a dataset of prior photo-based sea otter surveys from across Alaska, which included 11,939 sea otter observations from 6,536 photos. These photos were used to simulate the range of habitat variations and conditions encountered during this survey. We labeled each photo with bounding boxes to identify individual otters. We cropped the bottom third of each image to generate continuous, non-overlapping coverage of transects at a 300 m (0.19 mi) swath width and to remove the potential for double counting individual sea otters between consecutive images.

To ensure a uniform training set, we sliced the images into 1024 x 1024 pixel tiles to reduce the loss of resolution associated with resizing images. We divided the dataset into train, test, and validation datasets in the ratio of 70%, 15%, and 15%, respectively. We trained the YOLOv5 model using the train and validation datasets, while the test dataset remained untouched to generate unbiased metrics of performance. We trained the model with a priority on recall (R = 0.792) to minimize possible false negatives. We controlled the precision of the model (P = 0.806) by using manual validation via *SeeOtter* to remove any false positives.

We applied the trained AI model to the 2022 survey images, and every potential sea otter was labeled. We then manually validated the model output using *SeeOtter* to remove any false positives. An analysis of the precision-recall curves generated by the training data displayed a leveling off in model performance at a confidence threshold of ~ 0.4 (see Appendix 1, Figure A1.1. for recall and precision curves). Dropping the threshold below 0.4 significantly increased the false positive rate, while only incrementally decreasing the false negative rate. Therefore, we manually verified every prediction with a confidence score ≥ 0.4 and labeled each prediction as correct, incorrect, or ambiguous. Ambiguous annotations were the result of poor image quality, glare, animal behavior, or blur, and could not be confidently confirmed during manual validation by a single observer. Any observation labeled as ambiguous underwent a validation vote by three independent observers from the survey team to provide a final designation of correct (object was a sea otter) or incorrect (object was not a sea otter).

Finally, we used photo meta-data to project the photo footprints onto a map, to develop a survey footprint as a metric of survey effort. Each observation within a photo was georeferenced with the image dimensions, to generate specific GPS coordinates for each individual sea otter detected.

Fundamental differences between the two photographic systems resulted in different processing times to acquire data. We developed this report using the MX-10 data from across the study area and Waldo XCam data only from Glacier Bay. We are still processing and analyzing the still imagery obtained across all Southeast Alaska, concurrent with the MX-10 and expect those results in the coming year.

2.5 Data Analysis

To analyze new data collected in 2022, we applied the same mechanistic spatiotemporal model used to optimize the survey design (Eisaguirre et al. 2021), which is a fundamental part of maintaining a dynamic optimized monitoring program (Williams et al. 2018). Mechanistic spatiotemporal models based on ecological diffusion have become well established for modeling changes in sea otter distribution, abundance, and carrying capacity (Williams et al. 2017, 2018, 2019, Lu et al. 2020, Eisaguirre et al. 2021, 2023), and offer several advantages over other approaches, such as increased precision in estimates and improved ecological forecasting (Hefley et al. 2017, Williams et al. 2017, Eisaguirre et al. 2023).

We accommodated the new data collection methods by slightly modifying the data model component in the hierarchical model presented by Eisaguirre et al. (2021, 2023). Fitting the

model requires discretizing the study area into a grid of $i = 1, \ldots, q$ 400×400 m cells. This resolution was chosen to be consistent with the resolution of historical observer-based surveys (Williams et al. 2017). However, the new photo-based methods can cover more or less than a single grid cell at a time due to the area covered by the images/video and slight deviations of the aircraft along the transects. Thus, similar to Lu et al. (2020), we added a sampling effort variable $A_{i,t}$, which was the proportion of the *ith* grid cell covered by the swath of images/video captured along a transect such that $y_{i,t} \sim \text{Binom}\left(N_{i,t}, A_{i,t}p_{i,t}\right)$, where $y_{i,t}$ is the count recorded and $p_{i,t}$ is the detection probability. We provide a full statement of the hierarchical statistical model in Appendix 2.

Detection likely varied spatially in 2022 due to the different photo-based methods implemented in Glacier Bay versus the rest of the region. We used a moment-matched informative prior based on estimates presented by Williams et al. (2017) for detection in Glacier Bay (Lu et al. 2020, Eisaguirre et al. 2021). To estimate detection for the remainder of the region, we restricted our sample of 29 intensive searches to 20 that contained more than one sea otter group (Bodkin and Udevitz 1999). The result of these intensive searches is an initial count that followed the observation process along transects, paired with a true count, which includes individuals that went undetected in the initial count due to diving behavior, for example. These data were then used analogously to the previous years with observer-based ISU data to estimate detection with a Beta-binomial sub model (Williams et al. 2017, Lu et al. 2020, Eisaguirre et al. 2021).

To fit the model to the baseline dataset analyzed by Eisaguirre et al. (2021) augmented with the data collected in 2022, we estimated the parameters in the model, as well as derived quantities such as total abundance and carrying capacity, with a custom Markov chain Monte Carlo (MCMC) algorithm implemented in R (Eisaguirre et al. 2021, R Core Team 2022). We used 18 independent MCMC chains of 1,000 iterations, discarding the first 500 for burn in, to obtain a sample of 9,000 iterations from the posterior distribution for estimation, which required approximately 3,000 CPU hours (~ 7 days of run time with all 18 chains run in parallel). To assess model fit we compared observed counts (across all surveys) to the posterior predictive distribution pointwise by computing the 95% credible interval for each observed count (Eisaguirre et al. 2021).

3. Results

We conducted aerial photographic sea otter surveys across the Southeast Alaska stock region from May 22 to June 17, 2022. Of these 27 survey days, we were unable to conduct surveys on three days due to duty day restrictions or transit days when the base of operations was moved to a new location. We were unable to survey on one day due to weather and another day due to scheduled maintenance. Surveys within Glacier Bay were conducted on August 3, 4, and 12, 2022, one survey stratum completed per day.

Across the broader Southeast Alaska region (excluding Glacier Bay), we flew 8,700 km (5,406 mi) of survey spread across 736 transect lines flown in approximately 124 hours of flight time. The actual length of transects flown was longer than the 7,471 km (4,642 mi) design because the observation team periodically made in-flight adjustments to safely cover the intended survey area (e.g., to follow the length of narrow fjords rather than flying back and forth the width) and when

flying the contour of the northern outer coast, the flight path around features and into bays was much more convoluted than expected based on the transect line.

3.1 Sensor Results

The initial survey protocol established a flight altitude of 267 m (875 ft) altitude to maintain a Waldo XCam swath width of 300 m (0.19 mi). We reduced the flight altitude to 213 m (700 ft) to improve the image resolution of the Waldo XCam's static images. This decreased altitude assisted the MX-10 by negating a significant amount of glare. The decreased altitude allowed for the MX-10 to trail closer behind the plane at 0.6 - 0.8 km (0.4 - 0.5 mi) and maintain a comparable swath width (345 m - 430 m) to that of the Waldo XCam (~ 300 m) (Table 1).

3.1.1 L3/Harris MX-10 Results from across Southeast Alaska

A total of 559 detections of sea otters were made consisting of lone sea otters to group sizes of up to 346 sea otters. The total number of detected sea otters was 4,890, which includes sea otters detected throughout each day's flight inclusive of detections on transect and during transit (e.g., from airport to transects, among transects). A total of 387 sea otter detections were made on-transect, ranging from single individuals up to a group size of 138 sea otters, resulting in a total of 2,116 sea otters observed on-transect (Figure 3; see Appendix 3, Figure A3.2 for example photos). Twenty-nine of the sea otter detections triggered intensive searches for estimating availability, capturing an additional 134 sea otters. Only 20 of the intensive searches yielded more than one otter, allowing them to be used to estimate detection in the analysis. Sea otter sightings were quite variable among supplemental 20 km community buffer areas; ranging from zero to groups of > 100 sea otters (Figure 4).

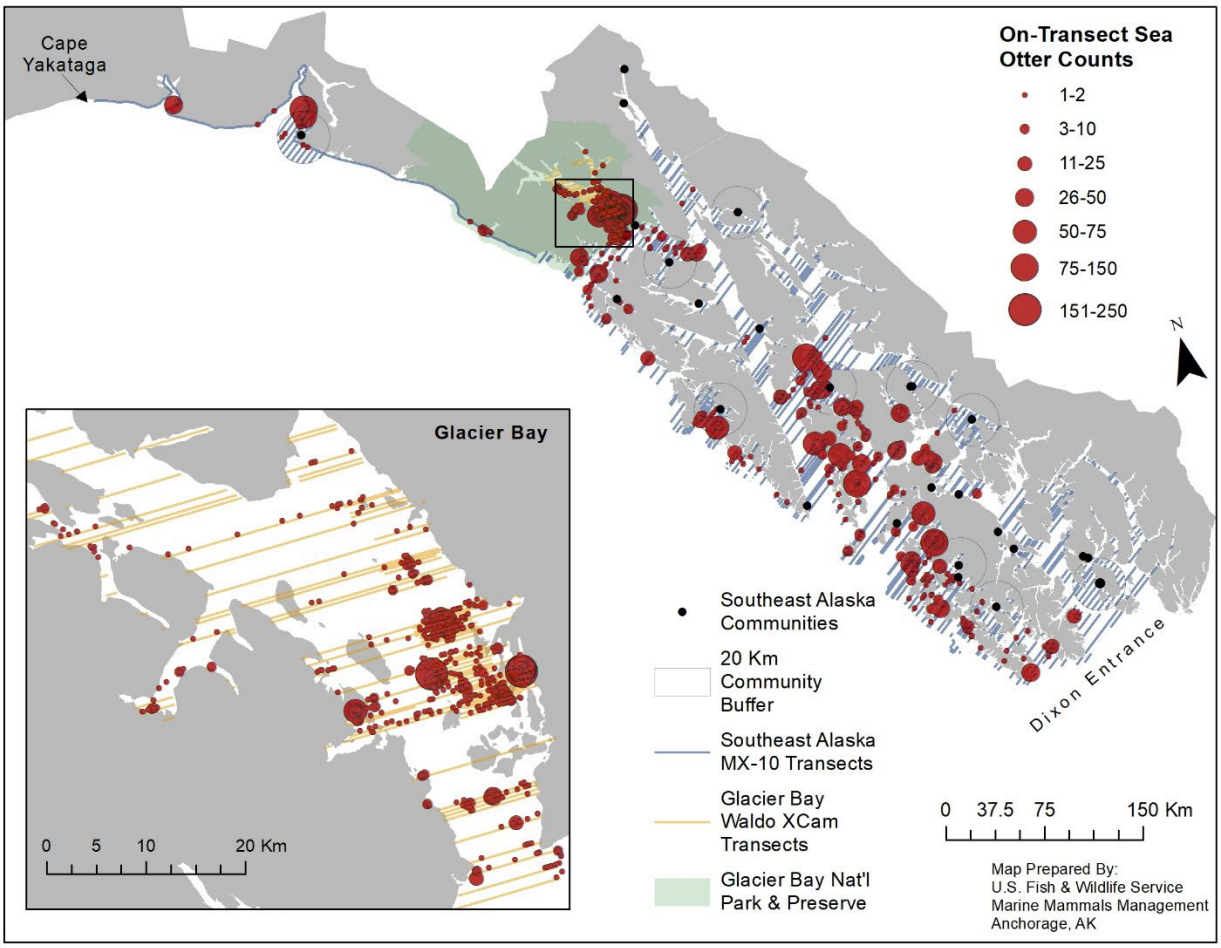

Figure 3. On-transect sea otter detections using the MX10 camera sensor across Southeast Alaska in 2022, scaled by group size from 1 to 250 sea otters (red points). Inset: On-transect sea otter detections using the Waldo XCam Ultra 50 and YOLOv5 AI algorithm from Glacier Bay.

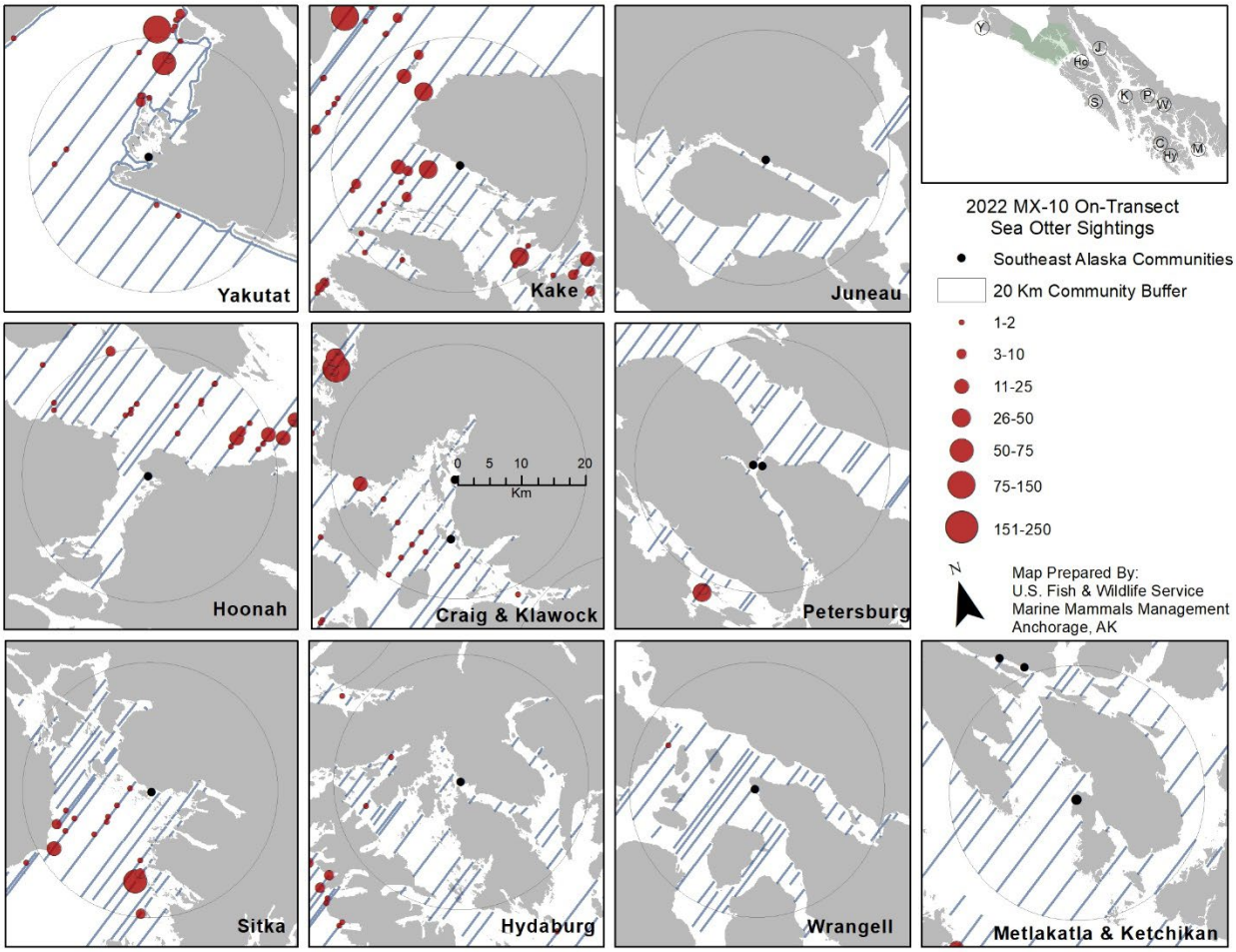

Figure 4. Zoomed in views from Figure 3 of on-transect sea otter detections using the MX-10 camera sensor within each of the ten, 20 km community buffer areas, across Southeast Alaska in 2022 (inset), scaled by group size from 1 to 250 sea otters (red points).

3.1.2 Waldo XCam Ultra 50 and Artificial Intelligence Algorithm Results from Glacier Bay

In Glacier Bay, 27,767 images were captured over 3 days in August (August 3, 4, and 12) combined across 3 survey strata, each flown a different day. Of those images, 19,223 were captured on transect resulting in a total of 2,685 sea otter predictions from the YOLOv5 AI algorithm that were validated to be correctly identified as sea otters by an expert-observer using *SeeOtter* (see Appendix 3, Figure A3.3 - A3.4 for screenshots of the software detecting sea otters). Sea otters were observed throughout much of Glacier Bay and the highest concentrations were observed in the lower and mid regions of Glacier Bay (Figure 3).

Across the study area outside of Glacier Bay, 279,539 images were captured between May 22 and June 17, 2022. We have so far manually validated 28,587 images using *SeeOtter* and the YOLOv5 algorithm and results from this data stream are expected later in 2023.

Table 1. Summary of the two camera sensors used for the Southeast Alaska sea otter population survey.

	MX-10	Waldo XCam
Region	Southeast except for Glacier Bay	Glacier Bay (this report); Southeast (in progress)
Imagery	Video, 2 sensors: IR & RGB	Photograph, 2 cameras: RGB
Capture Rate	Continuous	Photos every 1.5 - 2.0 seconds
Swath Width	345 - 430 m	300 m
Viewshed Time	~ 8 seconds	Instantaneous
View Perspective	Trapezoidal, oblique only with scanning capability	Rectangular, nadir perspective only and fixed
View Timing	Trailing, observationally 30 seconds behind the plane	Photographing directly beneath the plane
Imagery Captured	140 hours of video	Photos from Glacier Bay: 27,767 total, 19,223 on-transect; Southeast: 279,539 total (in progress)
In-flight Detection and Verification	Detection using IR and RGB video, verification of sightings using RGB live-video feed	None in-flight. Photo is instantly captured for later review. All detection and verification in post-processing using *SeeOtter*
Total Observations	4,890 total sea otters (including observations during transit)	2,685 total sea otters in Glacier Bay; Southeast (in progress)
On Transect Observations Used for Analysis	2,116 on-transect + 134 intensive search sea otters	2,508 on-transect sea otters in Glacier Bay; Southeast (in progress)

3.2 Spatiotemporal population model results

The survey design was optimized to maximize precision in equilibrium differential (or difference between local carrying capacity and local abundance). Applying the model to the baseline dataset augmented with the 2022 survey data resulted in increased precision in estimated total carrying capacity and total abundance compared to recent applications of the model only to the baseline dataset (e.g., Eisaguirre et al. 2021, 2023), suggesting the optimization procedure fulfilled its goal. Further, 99% of the observed counts (across all surveys) fell within the 95% posterior predictive intervals, suggesting no lack of fit of the model. Estimates of the parameters and overall population process are presented in Table 2.

Estimated total abundance of sea otters shows a relatively steady increase since translocations in the 1960's (Figure 5). Although there is substantial overlap in the credible intervals between years, estimated abundances during the most recent years with data were slightly lower than previous years when abundance was estimated only using the posterior predictive distribution (i.e., for years during which no data were collected). The estimate for total carrying capacity is lower than previous estimates, although more precise, but still reasonable, given the uncertainty

around those previous estimates (e.g., Tinker et al 2019: 95% Bayesian credible interval: 36,778, 136,506; Eisaguirre et al. 2023: 90% Bayesian credible interval: 54,063, 89,922).

Additionally, estimates of occupancy probability, obtained following Williams et al. (2019), suggest sea otters now occupy a majority of the stock region (Figure 6), and occur at varying densities (Figure 7). These metrics were computed at 400 m^2 resolution and aggregated to 1 km^2 for presentation.

The total estimated abundance (posterior mean and 95% credible interval) of sea otters in Southeast Alaska for 2022 is 22,359 (19,595, 25,290, CV = 0.064) (Table 3). Sea otter densities are highest in Glacier Bay, where they range up to 26.49 sea otters/km^2 (Figure 7). Outside of Glacier Bay, estimated densities are an order of magnitude lower, ranging up to 2.72 sea otters/km^2 (Figure 7). Additionally, as specified in the model due to the different photo systems used, detection was estimated to be higher in Glacier Bay than elsewhere, ranging from 0.57 (90% Bayesian credible interval: 0.52, 0.62) in areas surveyed with the MX-10 to 0.77 (95% Bayesian credible interval: 0.67, 0.85) in areas surveyed with the Waldo XCam (i.e., in Glacier Bay).

The estimated total carrying capacity (K) of sea otters in Southeast Alaska is 48,083 (40,575, 58,570) (Table 3). Estimated sea otter local carrying capacity in Glacier Bay ranges up to 29.99 sea otters/km^2. Estimated local carrying capacity in the remainder of Southeast Alaska ranges up to 9.82 sea otters/km^2 (Figure 8).

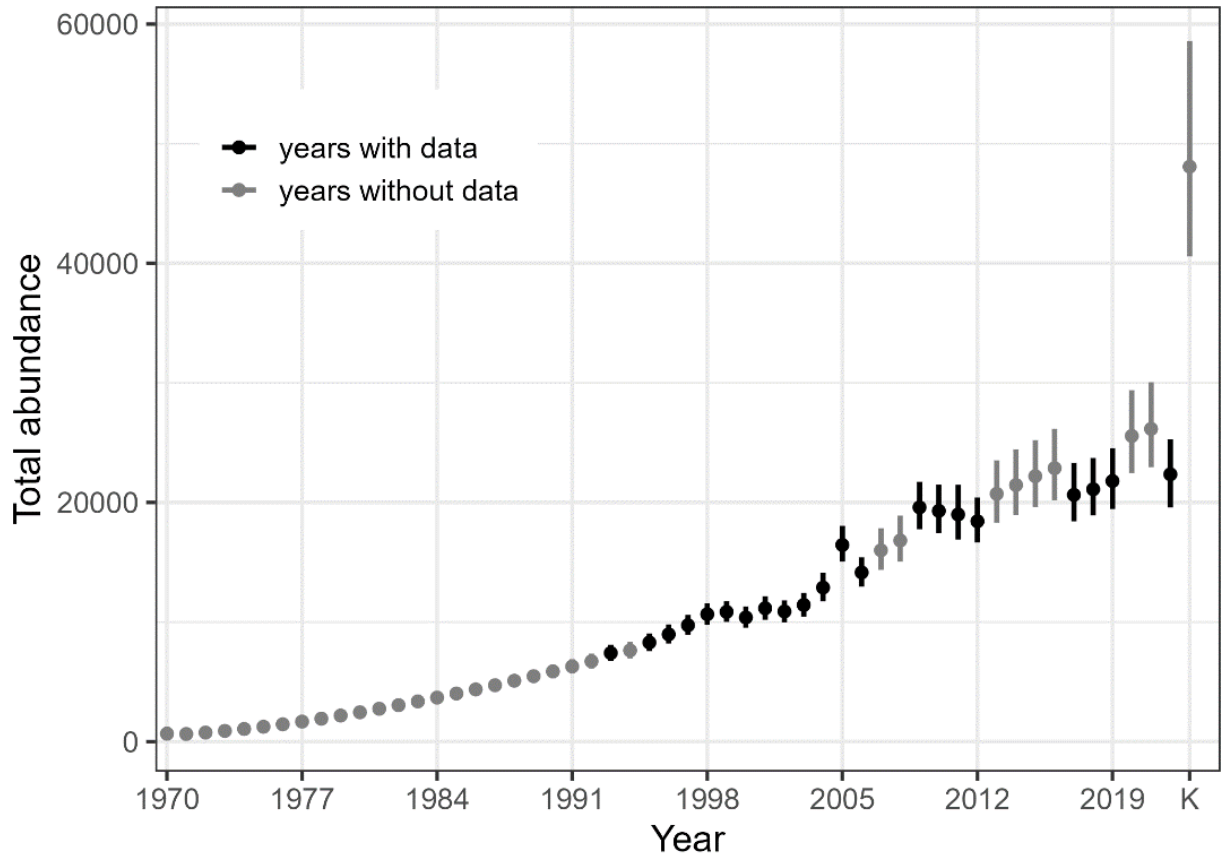

Figure 5. Estimated sea otter abundance 1970 – 2022 for the Southeast Alaska stock, including years when either abundance or distribution surveys were conducted (dark) and when surveys were not conducted (gray). The estimated carrying capacity (*K*) is indicated at right as 48,083 (40,575, 58,570).

Table 2. Posterior means and 90% Bayesian credible intervals for the parameters estimated in the mechanistic spatiotemporal model applied to the Southeast Alaska stock of sea otters. Note: P_{2022} within Glacier Bay was 0.77 (0.67—0.85) as with prior photo survey years (2017-2019).

parameter	lower bound	mean	upper bound
β_0 (intercept)	16.16	16.34	16.51
β_1 (depth)	-2.16	-2.03	-1.91
β_2 (distance to shore)	0.41	0.48	0.55
β_3 (slope × depth)	0.16	0.24	0.31
β_4 (shoreline complexity)	0.03	0.07	0.10
β_5 (distance to towns)	-0.53	-0.40	-0.29
β_6 (Glacier Bay)	0.01	0.19	0.40
β_7 (fisheries closures)	-1.64	-1.50	-1.33
α_0 (intercept)	-1.94	-1.83	-1.72
α_1 (Glacier Bay)	3.39	3.66	3.95
α_2 (fisheries closures)	-0.12	0.41	0.96
γ (intrinsic growth)	0.27	0.28	0.29
τ (overdispersion)	0.02	0.03	0.03
θ_{MI} (initial density)	35.98	45.31	143.59
θ_{BI}	1.27	2.62	8.86
θ_{NI}	5.77	9.75	13.32
θ_{KB}	2.83	10.78	92.13
θ_{YB}	0.79	2.33	9.00
θ_{YI}	4.88	14.66	84.72
θ_{CS}	19.25	27.61	121.10
κ_{MI} (initial dispersal)	35.98	37.65	39.46
κ_{BI}	1.27	2.14	3.07
κ_{NI}	5.73	9.74	13.36
κ_{KB}	2.83	4.45	5.40
κ_{YB}	0.78	1.81	2.89
κ_{YI}	4.76	8.91	12.04
κ_{CS}	19.24	20.34	21.37
p_{1993} (detection probability)	0.25	0.60	0.90
p_{1995}	0.24	0.60	0.91
p_{1996}	0.25	0.60	0.90
p_{1997}	0.24	0.60	0.90
p_{1998}	0.25	0.60	0.91
p_{1999}	0.34	0.52	0.70
p_{2000}	0.55	0.69	0.81
p_{2001}	0.67	0.78	0.87
p_{2002}	0.72	0.80	0.86
p_{2003}	0.60	0.66	0.71
p_{2004}	0.60	0.66	0.72
p_{2005}	0.27	0.34	0.41
p_{2006}	0.61	0.66	0.71
p_{2009}	0.25	0.60	0.91
p_{2010}	0.85	0.88	0.91
p_{2011}	0.25	0.60	0.91
p_{2012}	0.47	0.56	0.64
p_{2017}	0.67	0.77	0.85
p_{2018}	0.67	0.77	0.85
p_{2019}	0.67	0.77	0.85
p_{2022}	0.52	0.57	0.62

Table 3. Posterior means of annual abundance and predicted carrying capacity of sea otters for the Southeast Alaska stock in 2022. Lower and upper bounds correspond to the 95% Bayesian credible interval.

year	lower bound	mean	upper bound
1970	406	667	1271
1971	501	644	821
1972	609	761	936
1973	740	904	1091
1974	883	1064	1264
1975	1043	1249	1471
1976	1226	1455	1694
1977	1437	1681	1941
1978	1656	1924	2205
1979	1897	2186	2492
1980	2159	2462	2798
1981	2424	2755	3104
1982	2704	3053	3415
1983	2990	3368	3772
1984	3297	3689	4105
1985	3617	4028	4465
1986	3930	4369	4850
1987	4253	4721	5220
1988	4591	5096	5630
1989	4948	5477	6027
1990	5313	5875	6464
1991	5710	6291	6903
1992	6106	6721	7365
1993	6760	7416	8104
1994	6956	7633	8357
1995	7569	8297	9058
1996	8212	8979	9813
1997	8938	9738	10603
1998	9788	10660	11578
1999	10023	10855	11747
2000	9528	10390	11297
2001	10199	11162	12156
2002	9977	10890	11814
2003	10456	11433	12436
2004	11741	12891	14113
2005	15048	16455	18048
2006	12961	14154	15422
2007	14372	16002	17846
2008	15045	16822	18902
2009	17763	19598	21724
2010	17437	19304	21488
2011	16905	19000	21482
2012	16668	18435	20422
2013	18307	20727	23528
2014	18963	21459	24422
2015	19618	22200	25219
2016	20182	22870	26162
2017	18434	20643	23317
2018	18928	21109	23723

year	lower bound	mean	upper bound
2019	19463	21795	24525
2020	22453	25564	29392
2021	22952	26154	30053
2022	19595	22359	25290
K	40575	48083	58570

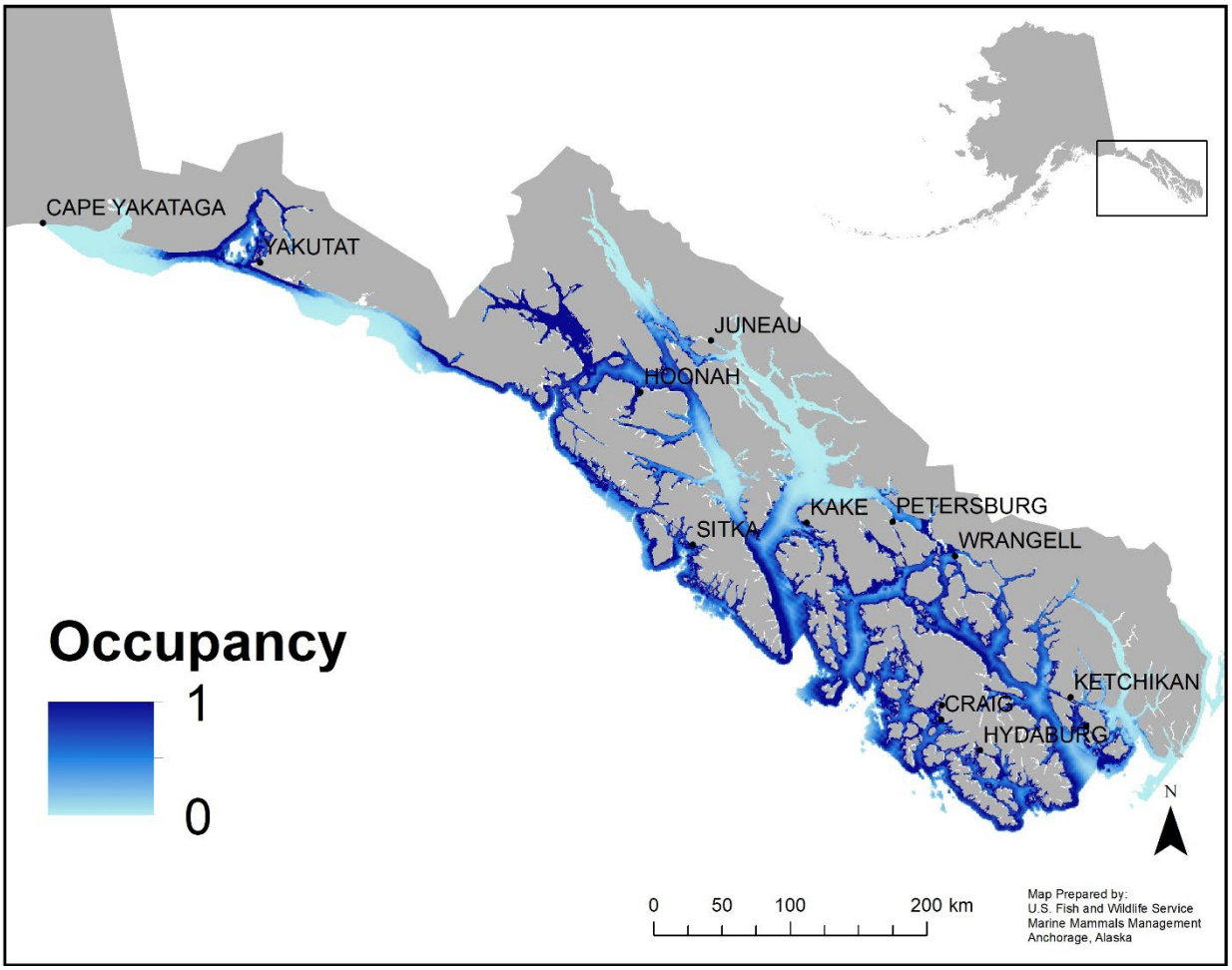

Figure 6. Estimated sea otter occupancy probability in 2022 based on the posterior mean from the mechanistic spatiotemporal model fit to all available aerial survey data collected in Southeast Alaska. Aggregated to a 1 km^2 grid for visualization.

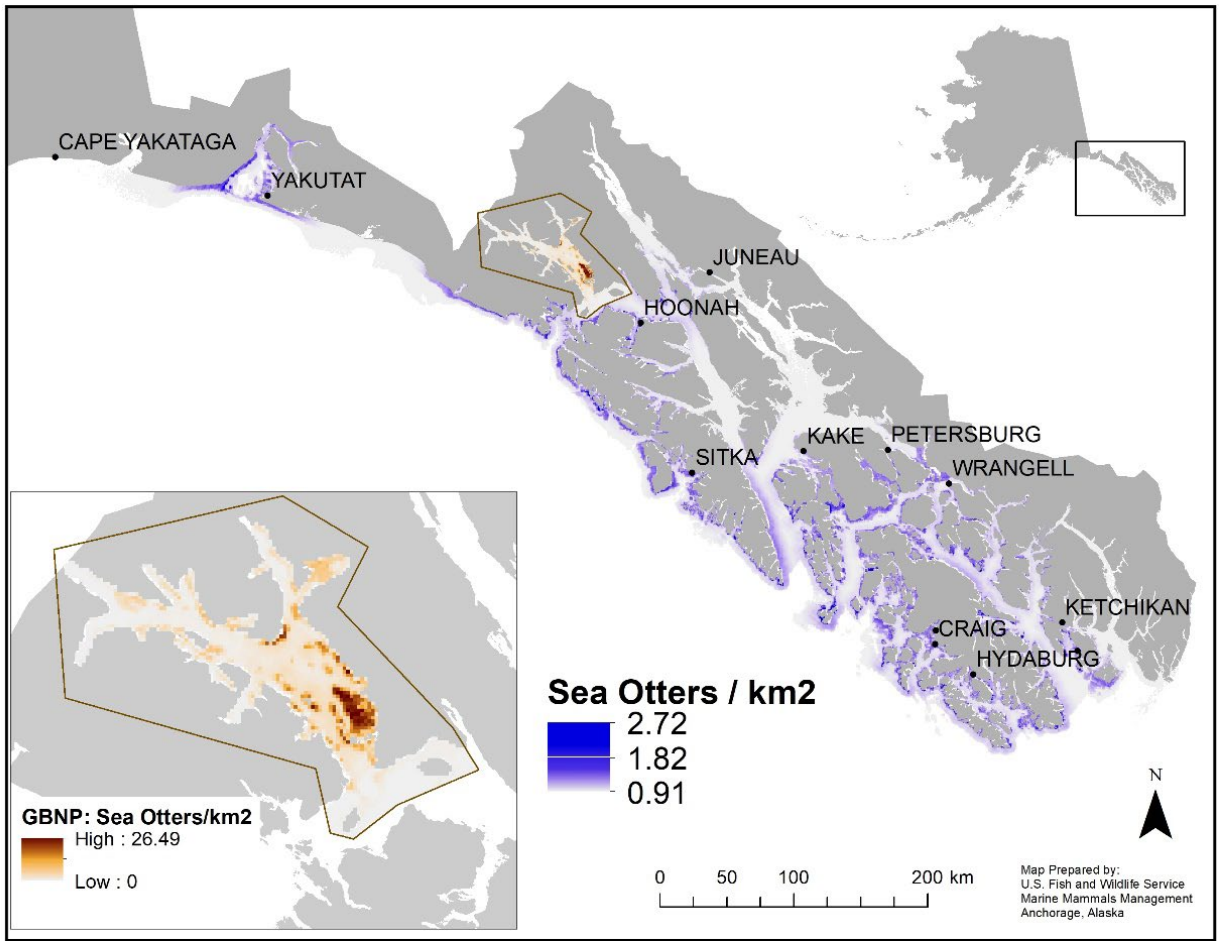

Figure 7. Estimated sea otter density in 2022 based on the posterior mean from the mechanistic spatiotemporal model fit to all available aerial survey data collected in Southeast Alaska. Aggregated to a 1 km^2 grid for visualization. The upper 95% posterior quantile of estimated density is available in Appendix 4, Figure A4.1.

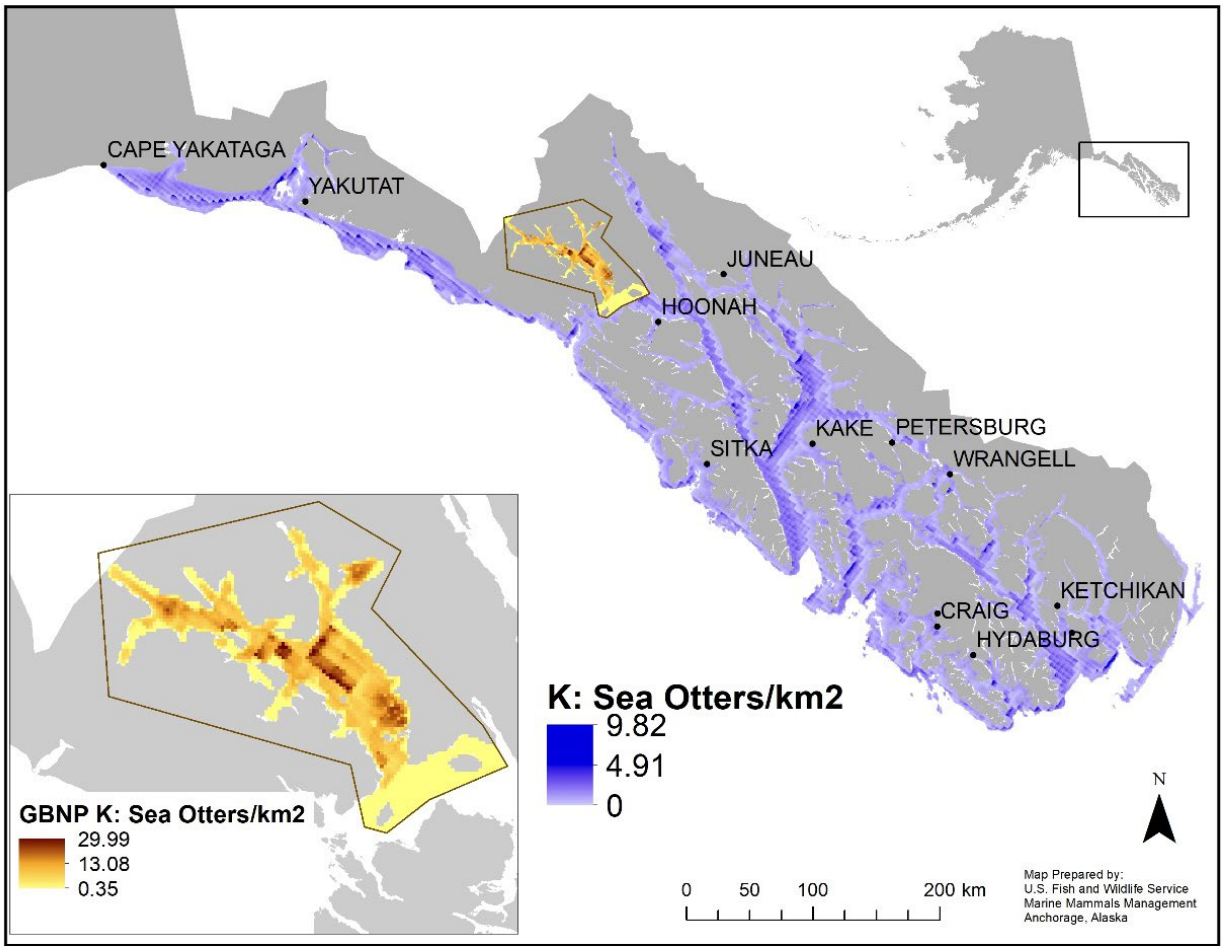

Figure 8. Estimated sea otter carrying capacity in 2022 based on the posterior mean from the mechanistic spatiotemporal model fit to all available aerial survey data collected in Southeast Alaska. Aggregated to a 1 km^2 grid for visualization. The upper 95% posterior quantile of estimated carrying capacity is available in Appendix 4, Figure A4.2.

4. Discussion

This photo-based aerial sea otter survey marks a substantial step forward in assessing sea otter abundance and distribution across Southeast Alaska. Photo-based aerial methods have previously gained traction for marine mammal population monitoring programs for their safety and effectiveness (Buckland et al. 2012), and after being adopted for sea otter population monitoring in Glacier Bay (Womble et al. 2020), we have now applied the technique at the scale of an entire stock. Owyhee Air Research provided technical support to conduct a sensor-based survey using the MX-10, high-end IR and RGB imaging system as a complement to the planned photo-survey using the Waldo XCam. We used recent advances in survey design optimization coupled with local and expert knowledge to prioritize and allocate survey effort in Glacier Bay National Park and Preserve, around local communities where subsistence users and commercial operators are based, and across the broader Southeast Alaska region. With the collected data, we used modern statistical modeling strategies to estimate current sea otter abundance at 22,359 (19,595, 25,290) and stock wide estimate of carrying capacity (K) at 48,083 (40,575, 58,570) sea otters. Our spatiotemporal population model also provides the added benefit of integrating all available historical sea otter survey data to allow us to estimate changes in sea otter population size and distribution through time as we continue to track sea otter recolonization following reintroduction.

4.1 Informing Sea Otter Management: Abundance and Carrying Capacity

The updated USFWS Stock Assessment Report for the Southeast Alaska stock uses a 2019 abundance estimate of 27,285 sea otters (Eisaguirre et al. 2021), which was based on Glacier Bay data through 2019 and regional data from a 2-year effort in 2010 and 2011, as well as all previously collected aerial survey data. Here, we have updated the model with empirical data gathered in 2022, which yielded a more precise but lower estimate of 2019 abundance at 21,795 sea otters. The most recent abundance estimate from 2022 in Southeast Alaska of 22,359 (19,595, 25,290) sea otters demonstrates a slowly increasing trend for the Southeast Alaska stock. Future updates to the Stock Assessment Report will use the best information available at the time of preparation. Further, trends for the stock should only be evaluated within population model results presenting annual abundance estimates, not between models (e.g., abundance estimates presented by Eisaguirre et al. 2021 or Eisaguirre et al. 2023 should not be compared to results presented in this report to infer population trends).

The 2022 sea otter population abundance estimate of 22,359 sea otters is approximately 46.5% of total estimated carrying capacity for the Southeast stock (K = 48,083 sea otters). These estimates of sea otter abundance and carrying capacity are subject to change with model refinement, improvement in or addition of new covariate data (e.g., improved bathymetry or ecological covariates), and inclusion of updated or alternate population surveys (e.g., future incorporation of Waldo XCam data across Southeast Alaska). However, the results presented in this report mark a step of progress and provide the latest estimates of sea otter abundance across the stock, given the current state of information. Further, the results suggests that large proportions of the stock region are not yet occupied by sea otters (Figure 6), contributing to the current difference between estimated stock-wide carrying capacity and abundance.

4.2 Optimized Survey Design

Monitoring programs that include dynamic optimized survey designs consist of a feedback loop between optimizing survey designs, collecting new data, fitting a statistical model to those new data (in addition to all "baseline" data) and optimizing a design for the next sampling period (Williams et al. 2018, Womble et al. 2018). The results of the survey presented here represent the first cycle in this loop for revising how sea otters are monitored in Southeast Alaska. While we did not detect a lack of fit for the underlying spatiotemporal population model, estimating lower abundances in recent years when data were collected, compared to years when no data were collected (Figure 3), suggests more frequent monitoring outside of Glacier Bay is likely required to accurately estimate abundance and trends across the entire stock moving forward. Given the mechanistic nature of the model, more frequent surveys over a rotation of smaller areas will likely result in better precision in parameter estimates and derived quantities (e.g., total abundance) than less frequent, stock-wide surveys.

The statistical survey optimization procedure, informed by the underlying continuous spatiotemporal population model, did not make any explicit assumptions about habitat quality. Rather, it let the data and process of ecological diffusion inform what areas should be sampled, and sea otters were detected during the 2022 survey in deep water (> 100 m) areas far from shore, which would have been excluded from sampling and analysis with a traditional design. Historically, those habitats were not surveyed to maximize efficiency of detecting sea otters where they are most likely to occur in a highly clustered manner and those habitats were deemed uninhabitable because sea otters could not forage and survive in those spaces. The traditional method for designing and conducting sea otter surveys in Alaska involved stratifying strip transects based on expected sea otter densities using a combination of depth and distance from shore. The high-density stratum was defined as water < 40 m deep or out to 400 m from shore, whichever is greater and the low-density stratum extends from 40 m to100 m deep or out to 2 km from shore, whichever is greater (Esslinger et al. 2021). Glacial fjords, bays, and inlets with entrances < 6 km wide are also designated as high-density habitat to reflect the tendency of resting sea otters to drift over deeper water in these areas. (Bodkin and Udevitz 1999). In contrast to the traditional abundance estimator (Bodkin and Udevitz 1999), contemporary spatially-explicit population models, like the spatiotemporal model we implemented, use both presence (e.g., counts of ≥ 1) and absence (i.e., counts of 0) information (Kéry and Royle 2016, Kéry and Royle 2020). Across our 2022 survey effort outside of Glacier Bay, > 50% of transect coverage included areas not previously considered for surveying, and while only ~ 7% of presence observations were made in those spaces (47 group sightings, totaling 170 sea otters) the abundance of absence information obtained along those transects better informs estimates of spatial distribution and density, and thus total abundance and carrying capacity as well. While there is potential for resting groups of sea otters, which can be highly concentrated and mobile with ocean currents, to occur over deeper waters and those observations may not have been observed in the traditional design-based surveys. Similarly, in a growing and expanding population, individuals or groups may occur in deeper water at higher frequency as they disperse to new areas, which we did detect at the margins of sea otter observations outside of Hoonah, Kake, and south of Wrangell (Figure 3). There were many areas that could have supported clusters of sea otters we did not survey in 2022 and future efforts across Southeast Alaska may

benefit from having strata specific to accounting for the clustering behavior of sea otter populations around shallow habitat, as observed in Glacier Bay (Womble et al. 2018).

4.3 Future Directions

We will continue to focus our attention on the status of sea otters across the Southeast Alaska stock. We are releasing this report with a current estimate of sea otter distribution, abundance, and carrying capacity to members of the Southeast Sea Otter Stakeholder Working Group and the public, and we welcome feedback. Similar to our survey design strategy, we would like to incorporate additional local knowledge and expert opinion as we continue to improve and refine our sea otter population model for the Southeast Alaska stock. Given that we collected two independent data streams, we plan to compare the accuracy and cost-effectiveness of the two methods. This effort will help inform methodological considerations for future photo-based sea otter population surveys.

This report focused on the MX-10 data from the broader Southeast Alaska region, but we will evaluate the total number of detections from the MX-10 (a high-end, expensive camera owned by OAR) in which sea otters were recorded in-flight by a camera operator relative to the Waldo XCam (an off-the-shelf system owned by USFWS and NPS) and our custom-built AI software. We will continue to evaluate the cost of using the two systems, the time investment to acquire sea otter data from imagery, personnel costs, and the accuracy of the resulting set of otter detections from the two strategies. Once the Waldo XCam data are prepared, reconciliation between the Waldo XCam and MX-10 data streams will yield another updated estimate of stock abundance and carrying capacity.

As we continue to refine the sea otter population model, we will also evaluate how we can more efficiently and regularly conduct sea otter population surveys. An advantage of the optimized survey design is that we can use our updated population models that include the 2022 data to explore where, how often, and when to conduct future surveys. This could include adoption of smaller scale, more frequent surveys, which could be done at a lower cost, be conducted by community members and other partners, and in general, help build collaboration and partnership across the broader Southeast region. We will continue to explore ways to make surveying sea otters more efficient, perhaps by incorporating strata (Womble et al. 2018) or considering depth contours (Schmidt et al. 2012). For example, inclusion of added covariates to account for uninhabitable habitat (e.g. occupiable waters > 100 m depth) will likely improve spatial predictions and lead to more efficient optimized designs in the future. Additional considerations of the physical environment (e.g., benthic substrate, categorized as rocky, soft, or mixed (Tinker et al. 2021)), ecological conditions (e.g. habitat, food availability), and anthropogenic activities (e.g., sea otter harvest, commercial fisheries, subsistence use of shellfish) could also help inform spatiotemporal patterns of sea otters in Southeast Alaska. We encourage readers to contact us about the utility of these ideas and other ideas to consider as we move forward. As the spatiotemporal model is refined and novel data are made available, we will continue to produce updated estimates of sea otter abundance and carrying capacity. Stock assessments will be updated as deemed necessary through reviews of the current state of information.

5. Acknowledgements

We appreciate the substantial support and guidance from the Southeast Sea Otter Stakeholder Working Group, Congressional representatives, and the numerous on-the-ground agency, university, tribal and community partners that helped make this survey a reality. Greg Rowe served as an exceptional pilot for the duration of this survey. We thank him and Owyhee Air Research for keeping us all safe in the sky. Chuck Schroth (Southeast Aerial) provided expert knowledge during logistical planning and safe aerial survey support for surveys in Glacier Bay. We anticipate the results from this project will lay the foundation for productive discussions, policy recommendations, and management decisions in the future. Survey design and logistics benefited from input by colleagues at the U.S. Geological Survey Alaska Science Center, namely Daniel Monson and Nicole Laroche. Early AI model development was supported by Charles Redmond from Mercyhurst University and Jeremy Greth, and statistical model refinement was supported by Perry Williams. Finally, we thank the U.S. Geological Survey Advanced Research Computing team for use of the Yeti Supercomputer (https://doi.org/10.5066/F7D798MJ).

The 2022 survey data and photo archive are available from the U.S. Fish & Wildlife Service, Marine Mammals Management, Anchorage, Alaska. This manuscript has been approved for publication consistent with USGS Fundamental Science Practices (http://pubs.usgs.gov/circ/1367/). Any use of trade, firm, or product is for descriptive purposes only and does not imply endorsement by the U.S. Government.

Our surveys spanned, Tlingit, Haida, and Tsimsian traditional territories. We extend our thanks, Gunalchéesh, Háw'aa, and Toyaxsut'nüün for their ongoing stewardship of these places since time immemorial.

6. Literature Cited

Bodkin, J. L. 2015. Historic and contemporary status of sea otters in the North Pacific. Page 447 *in* S. E. Larson, J. L. Bodkin, and G. R. VanBlaricom, editors. Sea Otter Conservation. Academic Press, London.

Bodkin, J. L., and M. S. Udevitz. 1999. An aerial survey method to estimate sea otter abundance. Pages 13–26 *in* G. W. Garner, S. C. Amstrup, J. L. Laake, B. F. J. Manly, L. L. McDonald, and D. G. Robertson, editors. Marine Mammal Survey and Assessment Methods. Balkema Press, Rotterdam, Netherlands.

Buckland, S. T., M. L. Burt, E. A. Rexstad, M. Mellor, A. E. Williams, and R. Woodward. 2012. Aerial surveys of seabirds: The advent of digital methods. Journal of Applied Ecology 49:960–967.

Burt, J. M., K.I.B.J. Wilson, T. Malchoff, S. H. A. Mack, W.T.K.A., Davidson, and A. K. Salomon. 2020. Enabling coexistence: Navigating predator-induced regime shifts in human-ocean systems. People and Nature 2:557–574.

Eisaguirre, J. M., P. J. Williams, X. Lu, M. L. Kissling, W. S. Beatty, G. G. Esslinger, J. N. Womble, and M. B. Hooten. 2021. Diffusion modeling reveals effects of multiple release sites and human activity on a recolonizing apex predator. Movement Ecology 9.

Eisaguirre, J. M., P. J. Williams, X. Lu, M. L. Kissling, P. A. Schuette, B. P. Weitzman, W. S. Beatty, G. G. Esslinger, J. N. Womble, and M. B. Hooten. 2023. Informing management of recovering predators and their prey with ecological diffusion models. Frontiers in Ecology and the Environment, in press.

ESRI. 2019. ArcMap 10.7.1. Environmental Systems Resource Institute, Redlands, California.

Esslinger, G. G. 2019. Sea Otter aerial survey data from Glacier Bay National Park and Preserve, 1999-2012: U.S. Geological Survey data release. Anchorage, Alaska.

Esslinger, G. G. 2020. Sea Otter aerial survey data from southeast Alaska, 2002-2003: U.S. Geological Survey data release. Anchorage, Alaska.

Esslinger, G. G., and J. L. Bodkin. 2009. Status and trends of sea otter populations in Southeast Alaska, 1969–2003: U.S. Geological Survey Scientific Investigations Report 2009–5045. Anchorage, Alaska.

Esslinger, G. G., D. Esler, S. Howlin, and L. A. Starcevich. 2015. Monitoring population status of sea otters (Enhydra lutris) in Glacier Bay National Park and Preserve, Alaska—Options and considerations: U.S. Geological Survey Open-File Report 2015-1119. Anchorage, Alaska.

Esslinger, G. G., B. H. Robinson, D. H. Monson, R. L. Taylor, D. Esler, B. P. Weitzman, and J. Garlich-Miller. 2021. Abundance and distribution of sea otters (Enhydra lutris) in the southcentral Alaska stock, 2014, 2017, and 2019: U.S. Geological Survey Open-File Report 2021–1122. Anchorage, Alaska.

Estes, J. A. and D. O. Duggins. 1995. Sea Otters and kelp forests in Alaska: generality and variation in a community ecological paradigm. Ecological Monographs 65:75–100.

Fedje, D. W., A. P. Mackie, R. J. Wigen, Q. Mackie, and C. Lake. 2005. Kilgii Gwaay: an early maritime site in the south of Haida Gwaii. Page 187e203 *in* D. W. Fedje and R. W. Mathewes, editors. Haida Gwaii: Human History and Environment from the Time of Loon to the Time of the Iron People. UBC Press, Vancouver, British Columbia.

Gill, V. A., and D. Burn. 2007. Aerial surveys of sea otters (Enhydra lutris) in Yakutat Bay, Alaska 2005. Technical Report: MMM 2007-01. Anchorage, Alaska.

Gorbics, C. S., and J. L. Bodkin. 2001. Stock structure of sea otters (Enyhdra lutris kenyoni) in Alaska. Marine Mammal Science 17:632–647.
Gregr, E. J., V. Christensen, L. Nichol, R. G. Martone, R. W. Markel, J. C. Watson, C. D. G. Harley, E. A. Pakhomov, J. B. Shurin, and K. M. A. Chan. 2020. Cascading social-ecological costs and benefits triggered by a recovering keystone predator. Science 368:1243–1247.
Hefley, T. J., M. B. Hooten, E. M. Hanks, R. E. Russell, and D. P. Walsh. 2017. Dynamic spatio-temporal models for spatial data. Spatial Statistics 20:206–220.
Hoyt, Z. 2015. Resource competition, space use and forage ecology of sea otters, Enhydra lutris, in southern southeast Alaska. University of Alaska Fairbanks.
Ibarra, S. N. 2021. Addressing a complex resource conflict: Humans, sea otters, and shellfish in southeast Alaska. Doctoral dissertation. University of Alaska Fairbanks.
Jameson, R. J., K. W. Kenyon, A. M. Johnson, and M. Howard. 1982. History and status of translocated sea otter populations in North America. Wildlife Society Bulletin 10:100–107.
Jocher, G., A. Chaurasia, A. Stoken, J. Borovec, NanoCode, Y. Kwon, K. Michael, TaoXie, J. Fang, Imyhxy, Lorna, 曾逸夫(zeng) Yifu, C. Wong, V. Abhiram, D. Montes, Z. Wang, C. Fati, J. Nadar, and … Jain Laughing. 2022. v7.0 - YOLOv5 SOTA Realtime Instance Segmentation.
Kenyon, K. W. 1969. The sea otter in the Easter Aleutian Paicific Ocean. North American Fauna 68.
Kery, M., and J. A. Royle. 2020. Applied hierarchical modeling in ecology: analysis of distribution, abundance and species richness in R and BUGS Volume 2: Dynamic and advanced models. Academic Press.
Kéry, M., and J. A. Royle. 2016. Applied hierarchical modeling in ecology: analysis of distribution, abundance, and species richness in R and BUGS. Academic Press, London.
Leach, C. B., P. J. Williams, J. M. Eisaguirre, J. N. Womble, M. R. Bower, and M. B. Hooten. 2022. Recursive Bayesian computation facilitates adaptive optimal design in ecological studies. Ecology 103:1–9.
Lu, X., W. P.J., H. M.B., P. J.A., W. J.N., and B. M.R. 2020. Nonlinear reaction–diffusion process models improve inference for population dynamics. Environmetrics 31:e2604.
Moss, M. L. 2020. Did Tlingit Ancestors Eat Sea Otters? Addressing Intellectual Property and Cultural Heritage through Zooarchaeology. American Antiquity 85:202–221.
R Core Team. 2022. R: A language and environment for statistical computing. R Foundation for Statistical Computing, Vienna, Austria.
Rasher, D. B., R. S. Steneck, J. Halfar, K. J. Kroeker, J. B. Ries, M. T. Tinker, P. T. Chan, J. Fietzke, N. A. Kamenos, B. H. Konar, and J. S. Lefcheck. 2020. Keystone predators govern the pathway and pace of climate impacts in a subarctic marine ecosystem. Science 369:1351–1354.
Salomon, A. K., K. B. J. Wilson, X. W. Elroy, N. Tanape Sr., and T. Mexsis Happynook. 2015. First Nations perspectives on sea otter conservation in British Columbia and Alaska: insights into coupled human-ocean systems. Page 447 *in* S. E. Larson, J. L. Bodkin, and G. R. VanBlaricom, editors. Sea Otter Conservation. Academic Press, London.
Schmidt, J. H., K. L. Rattenbury, J. P. Lawler, and M. C. Maccluskie. 2012. Using distance sampling and hierarchical models to improve estimates of Dall's sheep abundance. Journal of Wildlife Management 76:317–327.
Szpak, P., T. J. Orchard, I. McKechnie, and D. R. Gröcke. 2012. Historical ecology of late

Holocene sea otters (Enhydra lutris) from northern British Columbia: Isotopic and zooarchaeological perspectives. Journal of Archaeological Science 39:1553–1571.
Tegner, M. J., and P. K. Dayton. 2000. Ecosystem effects of fishing in kelp forest communities. ICES Journal of Marine Science 57:579–589.
Thometz, N. M., M. M. Staedler, J. A. Tomoleoni, J. L. Bodkin, G. B. Bentall, and M. T. Tinker. 2016. Trade-offs between energy maximization and parental care in a central place forager, the sea otter. Behavioral Ecology 27:1552–1566.
Tinker, M. T., V. A. Gill, G. G. Esslinger, J. Bodkin, M. Monk, M. Mangel, D. H. Monson, W. W. Raymond, and M. L. Kissling. 2019. Trends and carrying capacity of sea otters in southeast Alaska. Journal of Wildlife Management 83:1073–1089.
Williams, P. J., M. B. Hooten, G. G. Esslinger, J. N. Womble, J. L. Bodkin, and M. R. Bower. 2019. The rise of an apex predator following deglaciation. Diversity and Distributions 25:895–908.
Williams, P. J., M. B. Hooten, J. N. Womble, G. G. Esslinger, and M. R. Bower. 2018. Monitoring dynamic spatio-temporal ecological processes optimally. Ecology 99:524–535.
Williams, P. J., M. B. Hooten, J. N. Womble, G. G. Esslinger, M. R. Bower, and T. J. Hefley. 2017. An integrated data model to estimate spatiotemporal occupancy, abundance, and colonization dynamics. Ecology 98:328–336.
Wilmers, C. C., J. A. Estes, M. Edwards, K. L. Laidre, and B. Konar. 2012. Do trophic cascades affect the storage and flux of atmospheric carbon? An analysis of sea otters and kelp forestspp. Frontiers in Ecology and the Environment 10:409–415.
Womble, J. N., P. J. Williams, W. F. Johnson, L. F. Taylor-Thomas, and M. R. Bower. 2018. Sea otter monitoring protocol for Glacier Bay National Park, Alaska: Version SO-2017.1. Natural Resource Report NPS/SEAN/NRR—2018/1762. Fort Collins, Colorado.
Womble, J. N., P. J. Williams, X. Lu, L. F. Taylor, and G. G. Esslinger. 2020. Spatio-temporal abundance of sea otters in Glacier Bay National Park from 1993 to 2018. NPS/SEAN/NRDS2020/1283. Fort Collins, Colorado.

7. Appendices

Appendix 1. Artificial Intelligence model estimates of recall and precision.

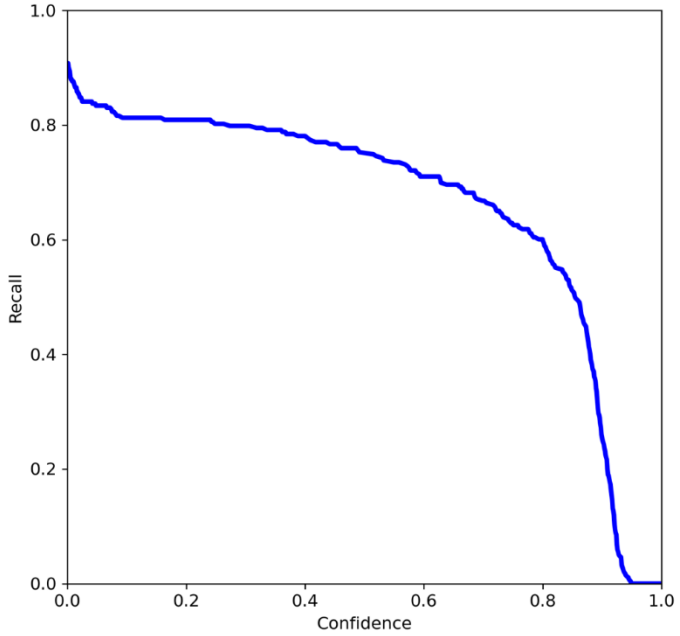

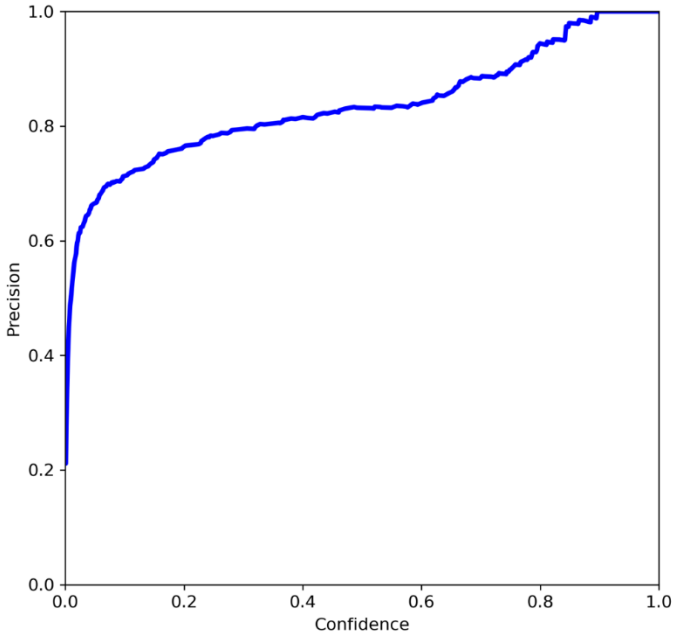

Figure A1.1. AI otter detection model performance at various confidence thresholds. Recall = True Positives / (True Positives + False Negatives); Precision = True Positives / (True Positive + False Positives).

Appendix 2. Statement of the hierarchical model.

Data Model:
$$y_{i,t} \sim \text{Binomial}(N_{i,t}, A_{i,t}p_{i,t}),$$

Process Model:
$$N_{i,t} \sim \text{NB}(\lambda_{i,t}, \tau),$$

$$\lambda_{i,t} = \int_{\mathcal{S}_i} u(\mathbf{s},t)d\mathbf{s}$$

$$\frac{\partial}{\partial t}u(\mathbf{s},t) = \left(\frac{\partial^2}{\partial s_1^2} + \frac{\partial^2}{\partial s_2^2}\right)\mu(\mathbf{s})u(\mathbf{s},t) + \gamma u(\mathbf{s},t)\left(1 - \frac{u(\mathbf{s},t)}{\kappa(\mathbf{s})}\right), \quad t > 1970$$

$$u(\mathbf{s},t) = \sum_{j=1}^{J} \frac{\theta_j e^{\frac{-|\mathbf{s}-\mathbf{d}_j|^2}{\nu_j^2}}}{\int_{\mathcal{S}} e^{\frac{-|\mathbf{s}-\mathbf{d}_j|^2}{\nu_j^2}} d\mathbf{s}}, \qquad t = 1970$$

$$\log(\mu(\mathbf{s})) = \beta_0 + \beta_1\text{depth}(\mathbf{s}) + \beta_2\text{dist}(\mathbf{s}) + \beta_3(\text{slope}(\mathbf{s}) \times \text{depth}(\mathbf{s})) + \beta_4\text{shore}(\mathbf{s}) + \beta_5\text{town}(\mathbf{s}) + \beta_6\text{glba}(\mathbf{s}) + \beta_7\text{fish}(\mathbf{s})$$

$$\log(\kappa(\mathbf{s})) = \alpha_0 + \alpha_1\text{glba}(\mathbf{s}) + \alpha_2\text{fish}(\mathbf{s})$$

Parameter Models:
$$p_{i,t} \sim \text{Beta}(3,2), \qquad t \neq 2017,2018,2019;\ i \notin \text{GLBA}$$

$$p_{i,t} \sim \text{Beta}(44.04937, 13.40566), \qquad t = 2017,2018,2019,2022;\ i \in \text{GLBA}$$

$$\tau \sim \text{Uniform}(0,1)$$

$$\boldsymbol{\beta} \sim \text{Normal}(\mathbf{0}, 10^2\mathbf{I})$$

$$\boldsymbol{\alpha} \sim \text{Normal}(\mathbf{0}, 10^2\mathbf{I})$$

$$\theta_j \sim \text{Normal}^+\left(\mu_{\theta,j}, \sigma^2_{\theta,j}\right), \qquad j = 1,2,\ldots,7,$$

$$\boldsymbol{\mu}_\theta = (100,10,10,100,10,100,100)',$$

$$\boldsymbol{\sigma}^2_\theta = (20^2,1^2,1^2,20^2,1^2,20^2,20^2)'$$

$$\nu_j \sim \text{Normal}^+(\mu_{\nu,j}, \sigma^2_{\nu,j}),$$

$$\boldsymbol{\mu}_\kappa = (10,2,10,10,2,10,10)',$$

$$\boldsymbol{\sigma}^2_\kappa = (3^2,1^2,3^2,3^2,1^2,3^2,3^2)'$$

Appendix 3. MX-10 and Waldo XCam example imagery.

Figure A3.1. Aerial surveys in Southeast Alaska (excluding Glacier Bay) were flown in the Owyhee Air Research P68C. Two camera sensors were attached to the aircraft: an L3/Harris MX-10 IR/RGB video system (bottom left) in the belly port and a Waldo XCam Ultra 50 (bottom right) under the front passenger seat.

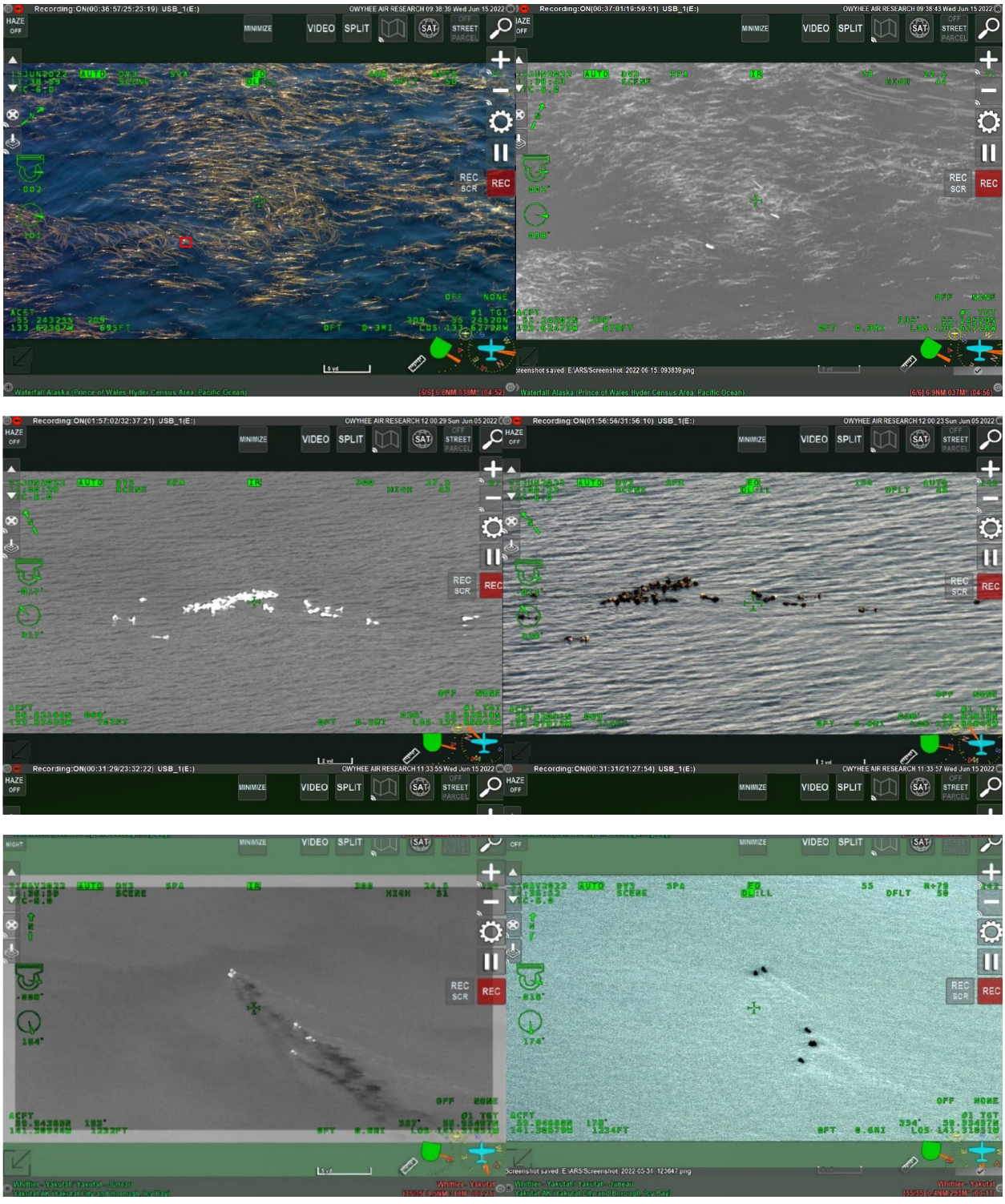

Figure A3.2. Example imagery from the Owyhee Air Research MX-10 sensor. These images are screenshots of the computer monitor in the P68C aircraft that were viewed continuously during flight. The operator searched a fixed width area with the infrared sensor to identify a heat signature and switched to RGB to zoom in/out, confirm whether the object(s) was a sea otter, and record a count.

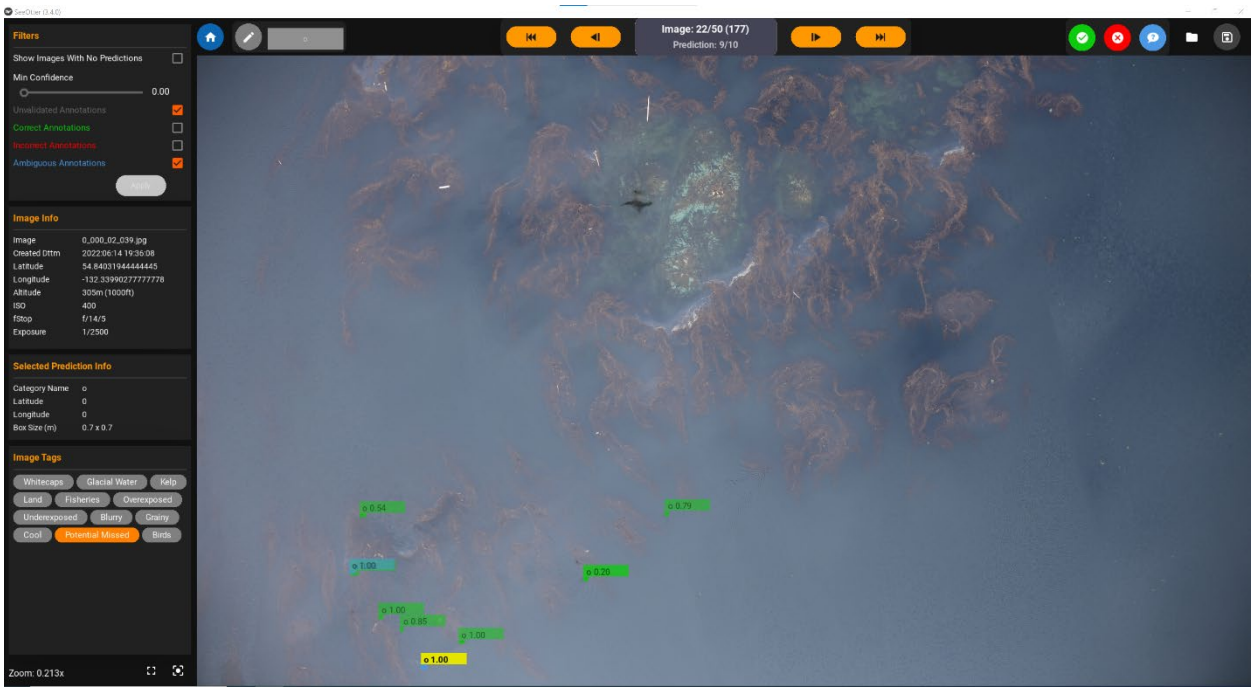
Filters
Show Images With No Predictions
Min Confidence
0.00
Unvalidated Annotations
Correct Annotations
Incorrect Annotations
Ambiguous Annotations
Apply
Image Info
Image 0_000_02_039.jpg
Created Dttm 2022:06:14 19:36:08
Latitude 54.84031944444445
Longitude -132.33990277777778
Altitude 305m (1000ft)
ISO 400
fStop f/14/5
Exposure 1/2500
Selected Prediction Info
Category Name o
Latitude 0
Longitude 0
Box Size (m) 0.7 x 0.7
Image Tags
Whitecaps
Glacial Water
Kelp
Land
Fisheries
Overexposed
Underexposed
Blurry
Grainy
Cool
Potential Missed
Birds
Zoom: 0.213x
Image: 22/50 (177)
Prediction: 9/10
o 0.54
o 0.79
o 1.00
o 0.26
o 1.00
o 0.85
o 1.00
o 1.00

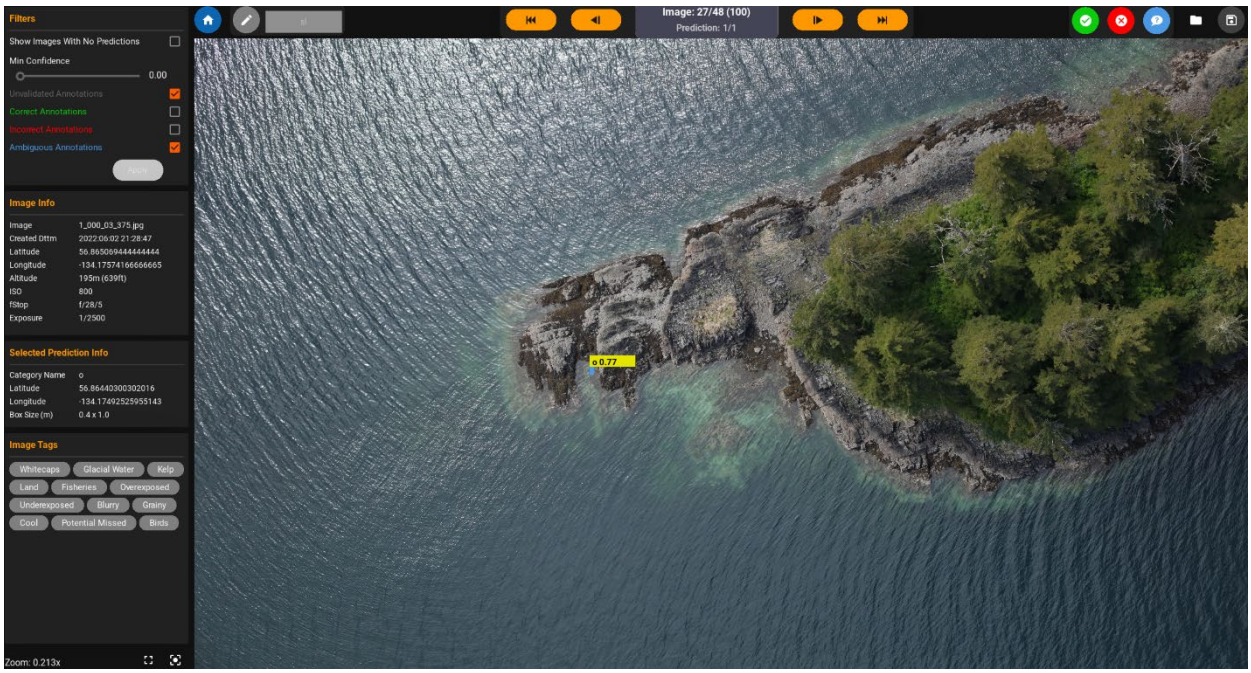
Filters
Show Images With No Predictions
Min Confidence
0.00
Unvalidated Annotations
Correct Annotations
Incorrect Annotations
Ambiguous Annotations
Apply
Image Info
Image 1_000_03_375.jpg
Created Dttm 2022:06:02 21:28:47
Latitude 56.865059444444444
Longitude -134.17574166666665
Altitude 195m (639ft)
ISO 800
fStop f/28/5
Exposure 1/2500
Selected Prediction Info
Category Name o
Latitude 56.86440300302016
Longitude -134.17492525955143
Box Size (m) 0.4 x 1.0
Image Tags
Whitecaps
Glacial Water
Kelp
Land
Fisheries
Overexposed
Underexposed
Blurry
Grainy
Cool
Potential Missed
Birds
Zoom: 0.213x
Image: 27/48 (100)
Prediction: 1/1
o 0.77

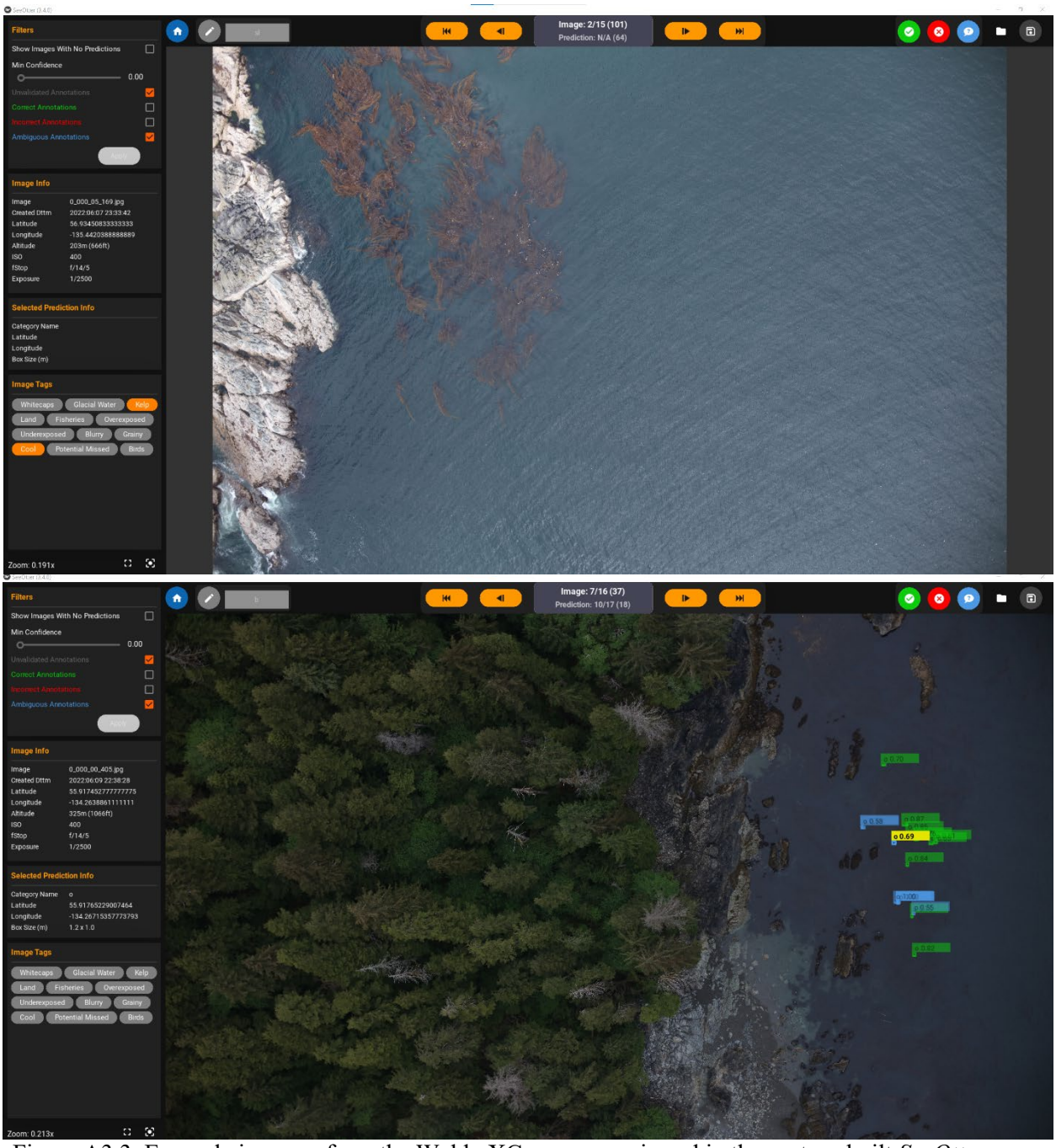

Figure A3.3. Example imagery from the Waldo XCam sensor viewed in the custom-built *SeeOtter* software (4 screenshots). The YOLOv5 model made predictions of potential sea otters in each image, which were then manually validated to confirm whether the detected object was a sea otter. The 3rd figure (above) shows the sea otters without the predictive bounding boxes to illustrate the relative size of sea otters while flying at an altitude of approximately 213 m (700 ft).

Appendix 4. Additional figures.

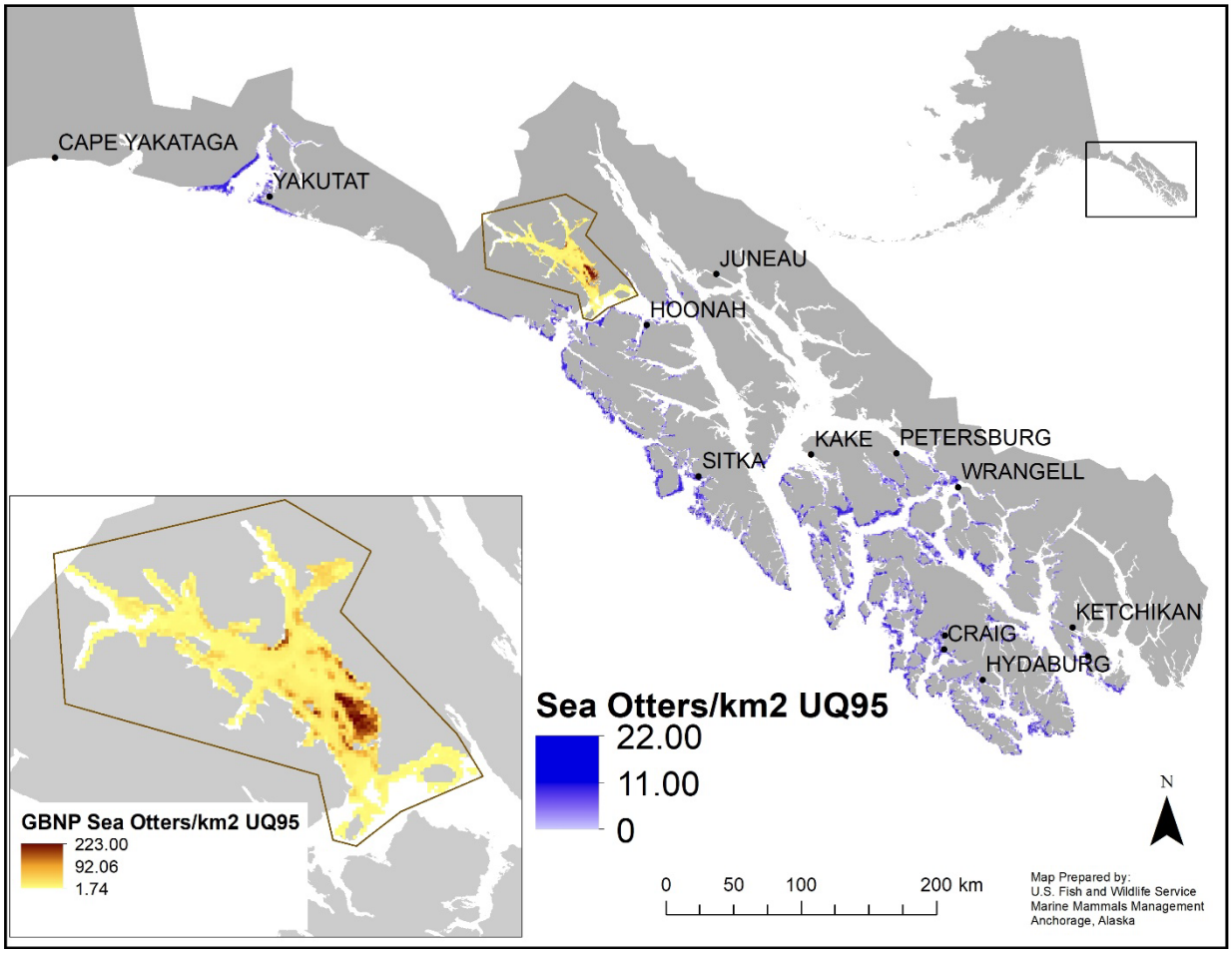

Figure A4.1. Upper 95% posterior quantile of estimated sea otter density in Southeast Alaska based on aerial surveys conducted in May and June 2022. This map depicts the highest densities (top 5%) predicted for 2022, aggregated to a 1 km^2 grid for visualization.

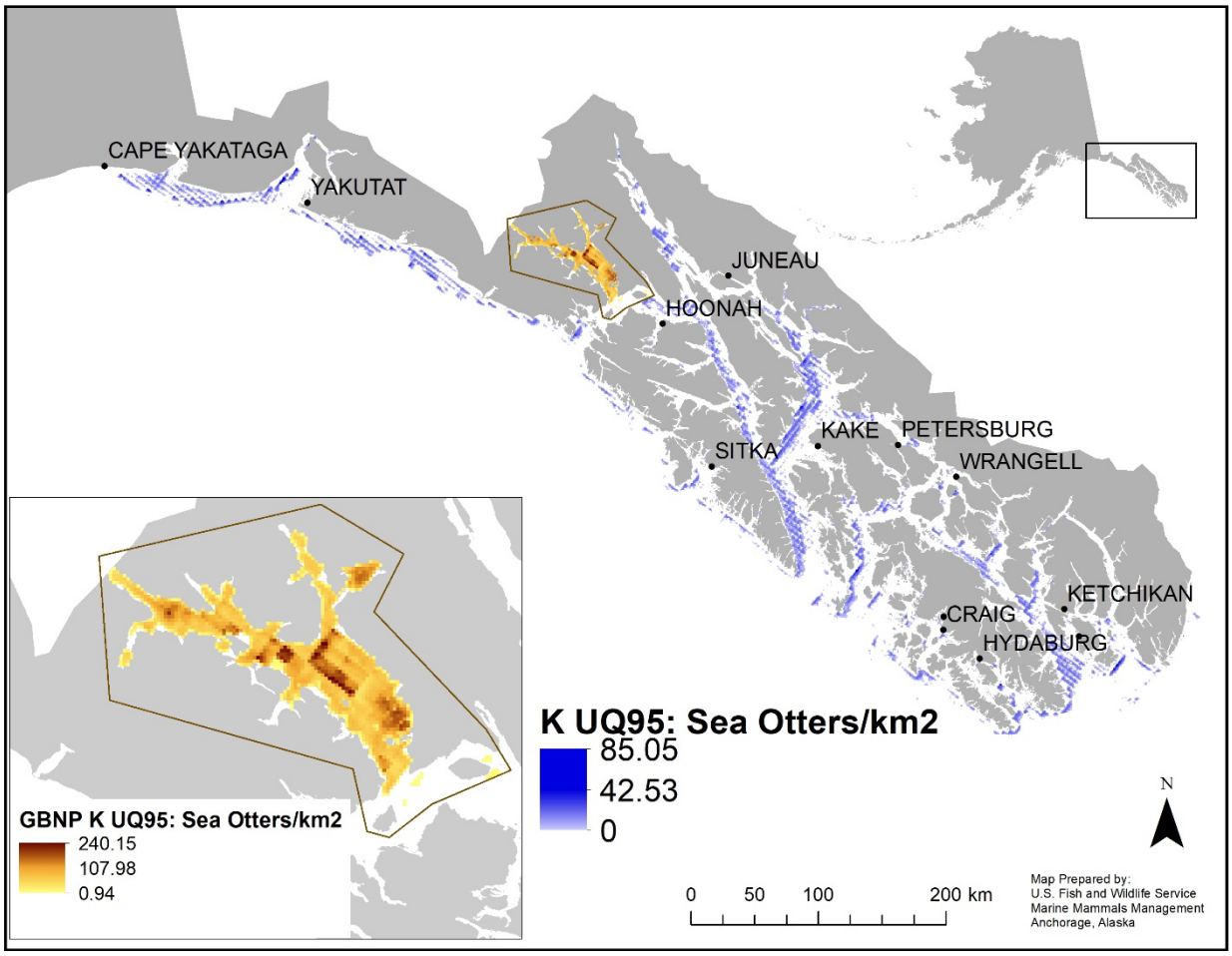

Figure A4.2. Upper 95% posterior quantile of sea otter carrying capacity in Southeast Alaska based on aerial surveys conducted in May and June 2022. This map depicts the highest estimated carrying capacity (top 5%) predicted for 2022, aggregated to a 1 km^2 grid for visualization.